Desalination and Water Treatment
www.deswater.com
doi: 10.1080/19443994.2013.870769

53 (2015) 1755–1779
February

Taylor & Francis
Taylor & Francis Group

Closed circuit desalination series no-9: theoretical model assessment of the flexible BWRO-CCD technology for high recovery, low energy and reduced fouling applications

Avi Efraty

Desalitech Ltd, P.O. Box 132, Har Adar 90836, Israel
Email: avi@desalitech.com

Received 3 June 2013; Accepted 17 October 2013

ABSTRACT

Compared with conventional BWRO techniques, The conceptually different closed circuit desalination technology for brackish water desalination (BWRO-CCD), has been analyzed with respect to its modular design and performance characteristics on the basis of theoretical model simulations of a typical four elements module (ME4; M = ESPA2-MAX) in the feed salinity range of 500–6,000 ppm NaCl, which corresponds to that of common brackish water sources with up to 7,000 ppm TDS. The model analysis results of the BWRO-CCD technology demonstrate a unique consecutive sequential desalination process with staged flow and pressure boosting without the use of staged pressure vessels and booster pumps. The theoretical model simulations of the BWRO-CCD technology over a wide range of feed salinity (500–6,000 ppm NaCl) have consistently revealed flexible and versatile performance under fixed flow and variable pressure conditions characterized by low energy consumption, high recovery, and reduced fouling characteristics achieved by means of simple designed systems of high modularity. The superb performance characteristics of the BWRO-CCD technology makes it ideal for a wide spectrum of noteworthy applications, such as treatment surface and groundwater for domestic use, desalination of clean domestic and industrial effluents, desalination of brackish water, production of high-quality permeates for industry, decontamination of drinking water including nitrate removal, boron removal from first-pass SWRO permeate, as well as many others. The theoretical model analysis results reveal that BWRO-CCD is an advanced technology which meets the criteria of high recovery and low energy consumption with reduced fouling in the simple apparatus of modular designs.

Keywords: Closed circuit desalination; CCD; High recovery; High flux; Low energy; Reduced fouling; Brackish water

1. Introduction

Water desalination has become increasingly important in reference to water supply for domestic, industrial, and agricultural applications in view of the rapidly growing global population and its increased standards of living, and in light of the declined availability of natural water sources due to depletion and/or deterioration of ground and underground water sources combined with the growing global "*green-house* effects" of adverse climate changes in various parts of the world. Desalination techniques apply nowadays to

various categories [1] of water sources of different salinity, such as seawater (15,000–50,000 ppm), brackish water (1,500–15,000 ppm), river water (500–3,000 ppm), pure water (<500 ppm), and wastewater of different origins, including treated and untreated domestic effluents (250–1,000 ppm) and industrial effluents (>1,000 ppm). Most of the currently practiced desalination techniques are based on reverse osmosis (RO) with clear distinction made between the well-defined seawater desalination techniques (SWRO) [2–5] and the widespread diverse brackish water desalination (BWRO) applications [1,5–8], many of which are considered in context of water treatment rather than desalination.

Although both conventional SWRO and BWRO are performed by single-pass plug flow desalination (PFD) techniques, the former is carried out in modules of seven and eight elements each with low recovery (40–50%) in a rather confined seawater salinity range of similar composition with effective energy recovery means from brine being a major issue; whereas, the latter applies for 75–90% recovery of wide salinity range sources using two or three staged pressure vessels designs commonly of six elements each, with inter-stage booster pump(s), or turbo-chargers to attain the desired recovery with sufficiently high energy efficiency. Although the production capacity of BWRO units tend be smaller compared with the super large, advanced SWRO plants installed during the past decade, the former technique in combination with other membrane technologies such as microfiltration, ultrafiltration, and nanofiltration plays an ever-growing role in municipal water treatment plants around the world, and this apart from their traditional role for the desalination of saline aquifers and recovery of industrial effluent for reuse. The diverse BWRO applications are directed to enormously large markets revealed, among other applications, by the need of second-pass desalination for most first-pass permeates produced by large SWRO plants in order to reduce the level of boron in the supplied water, and this exemplifies extensive BWRO needs even in the context of such large SWRO plants.

The most common problem encountered with conventional BWRO techniques relates to fouling of membranes and the need to apply cleaning procedures (CIP– clean in place) to restore their effectiveness with an increased need for CIP adversely effecting the performance of membranes. Fouling of membranes may be due to particulate matter in the feed and/or may originate from bacteria growth on membrane surfaces (bio-fouling) and/or by scaling of low-solubility precipitates (e.g. $CaCO_3$, $CaSO_4$, $BaSO_4$, silicates, etc.), many of which cannot be removed even by rigorous CIP procedures. In general, scaling is a major common problem in most high recovery BWRO applications, whereas both SWRO and BWRO are prone to bio-fouling to about the same extent and consequently, manuals of membrane producers [9] devote considerable attention to the various theoretical and practical aspects of membranes' fouling.

Conventional RO is a PFD technology based on hydrodynamic principles which remained essentially unchanged since inception in the late early 1960s by Loeb and Sourirajan [10], except for major improvement of semi-permeable membranes and energy recovery means. During the past year, several publications have described new RO technologies of closed circuit desalination (CCD) by means of consecutive sequential batch processes and their applications for seawater desalination (SWRO-CCD) [11–14] and for (BWRO-CCD) [15–19]. The new CCD technologies are performed under fixed flow and variable pressure conditions with high recovery determined only by the maximum applied pressure of operation irrespective of the number of elements per module, low energy of near theoretical minimum without need for energy recovery means, and reduced fouling and bio-fouling characteristics. The current paper describes a uniform approach to the design of simple modular BWRO-CCD systems of high recovery, low energy consumption, and reduced fouling tendencies and analyzes their flexible performance characteristics on the basis of theoretical models as compared with experimental results.

2. Single-module BWRO-CCD ME*n* (*n* = 1–6) unit design and operation

The conceptual approach to the proprietary BWRO-CCD technology [20] is illustrated in the schematic design displayed in Fig. 1 with an apparatus of the ME*n* (*n* = 4) configuration comprising a single pressure vessel with four elements and some free space, a high pressure pump (HP) with variable frequency derive (vfd), a circulation pump (CP) with vfd, an actuated valve (AV), and a check valve (OWV, one-way valve) means for occasional replacement of brine by fresh feed inside the closed circuit without stopping desalination. The apparatus also comprise monitoring means of flow, pressure and electric conductivity (EC) of the recycled concentrates, feed and permeate as appropriate for the control of the process. The apparatus in Fig. 1 and apparatus alike with more or with less elements per pressure vessel may be used for continuous consecutive sequential desalination of brackish water by a two-step (CCD-PFD) process with CCD performed under fixed flow and variable pressure conditions experienced most of the time and followed by brief PFD steps for periodic replacement of brine by fresh feed inside the closed circuit when the

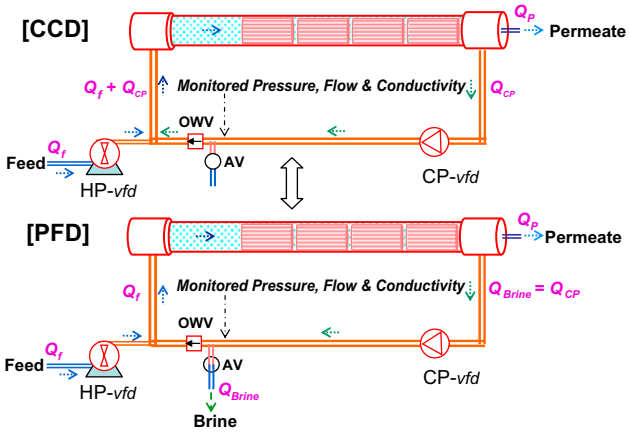

Fig. 1. A single module apparatus of the MEn (n = 4) configuration for a continuous BWRO-CCD operation by a two step consecutive sequential process.

desired recovery level is attained. The preferred module design with of four elements is no coincidence since longer modules (n > 4) also imply the lower production contributions of tail elements combined with a declined average flux and increased fouling probability; whereas, modules of four elements could be operated with a relatively higher average flux and enable similar overall production expected of longer modules with better quality permeates and lower fouling probability. In some cases of low salinity feed with low scaling constituents, the high recovery applications of the BWRO-CCD technology with modules of 5 and even six elements is not unreasonable.

The actuation of the apparatus displayed in Fig. 1 proceeds by controlled board selection of operational set points (SPs) associated with CCD, such as pressurized feed flow (Q_f), cross flow (Q_{CP}), and maximum applied pressure (p_{max}), as well as with PFD SPs such as a different pressurized feed flow or the same as before, brine replacement flow (QBrine), and brine replaced volume (V_{Brine}). The CCD step will continue with fixed flow rates under variable applied pressure conditions until the attainment of p_{max} which manifests the desired recovery and triggers the CC → PFD formation by the opening of the AV valve means. The PFD step proceeds with accelerated feed flow and reduced module recovery (MR) compared with CCD and the termination of this step with resumption of CCD takes place when the replaced brine volume from the closed circuit matches the volumetric SP(V_{Brine}). The preferred sequential period comprises CCD during 85–90% of the time and PFD during the remaining period, with the latter taking place under reduced pressure in order to minimize loss of energy during the brine replacement step. Some of the control SPs may be replaced by other monitored parameters such as maximum salinity of recycled concentrates instead of maximum applied pressure. The BWRO-CCD process under review can be optimized "on-line" by an infinite number of SPs combinations which cover all the aspects of process, including the membranes' performance.

The PFD steps of the consecutive sequential process are fully characterized by means of the conventional RO theory with flow balance expressed by Eq. (1), applied pressure (p_{appl}) by Eq. (2), and permeate salinity (C_p) by Eq. (3), wherein μ stands for flux, A for permeability coefficient, T_{CF} for temperature correction factor, $\Delta\pi_{av}$ for average concentrate-side osmotic pressure difference, Δp for module inlet/outlet pressure difference, p_p for permeate release pressure, π_p for average permeate-side osmotic pressure, B for diffusion coefficient, C_f for feed concentration, and pf_{av} for average concentration polarization factor (beta). The average concentration polarization factor can be expressed by Eq. (4), wherein Y_{av} stands for the average element recovery expressed by Eq. (5) with MR being the module recovery (%) and n the number of elements per module. Concentrate-side pressure drop [Δp(bar)] in 8" pressure vessels may be expressed by Eq. (6), wherein q stands for the arithmetic average concentrate-side flow (m^3/h) expressed by Eq. (7) and the exponent factor z for the characteristic flow features inside the selected element.

$$Q_f = Q_p + Q_{Brine} \tag{1}$$

$$p_{appl} = \mu/A/TCF + \Delta\pi_{av} + \Delta p/2 + p_p - \pi_p \tag{2}$$

$$C_p = B \times C_f \times pf_{av} \times T_{CF}/\mu \tag{3}$$

$$pf_{av} = 10^{k \times Y_{av}} \tag{4}$$

$$Y_{av} = 1 - (1 - MR/100)^{1/n} \tag{5}$$

$$\Delta p(bar) = (8/1,000) \times n \times q^z \tag{6}$$

$$q(m^3/h) = (1/2) \times (\text{module inlet flow} + \text{module outlet flow}) \tag{7}$$

The CCD steps of the consecutive sequential process are operated under fixed flow (Q_f and Q_{CP}) and variable pressure conditions without release of brine, and this implies the same feed flow and permeates flow (Q_f = Q_p), module inlet flow of Q_f + Q_{CP}, and module outlet flow of Q_{CP}. Under the fixed flow conditions during CCD, the salinity of the recycled concentrates is increased as function of recovery and this implies an increase in the sequentially applied

pressure (p_{appl}), mainly due to increase of $\Delta\pi_{av}$ and this effects increase of permeates' salinity (Cp) since the feed to the module is also a function of the recycled concentrates. The CCD cycles of the consecutive sequential process are well defined from the theoretical stand point with recovery (R) expressed by Eq. (8), wherein V stands for the fixed free intrinsic volume of the closed circuit and v for the volume of permeates produced during a CCD sequence - v is identiical to the feed intake since $Q_f = Q_p$. Since CCD proceeds with fixed feed flow (Q_f) under variable pressure conditions with an average sequential applied pressure expressed by p_{av}, the volume term v may be expressed by Eq. (9), wherein T stands for the time duration of the CCD sequence. Substituting the v expression derived from Eq. (8) into Eq. (9) yields Eq. (10) which establishes the relationships between R, T, V, and Q_f (=Q_p). The module recovery (MR) during the CCD cycles of the process in the apparatus displayed in Fig. 1 is expressed by Eq. (11) and depends only on the SPs' selection of the flow rates Q_f(HP) and Q_{CP}(CP), and the ability to select the MR also implies control of the head element recovery (HER). The specific energy (SE) terms during the CCD sequence are expressed by Eqs. (12) and (13) for HP and CP, respectively, with total RO energy demand (SE_{total}) expressed in Eq. (14) by the sum of the individual terms, wherein f_{HP} and f_{CP} stand for the efficiency factors of the respective pumps and Δp for the module inlet/outlet pressure difference.

$$R(\%) = [v/(v+V)] \times 100 \tag{8}$$

$$v = Q_f \times T = Q_p \times T \,\text{Since}\, Q_f = Q_p \tag{9}$$

$$T = R \times V/[Q_f \times (100 - R)] = R \times V/[Q_p \times (100 - R)] \tag{10}$$

$$MR(\%) = Q_f \times 100/(Q_f + Q_{CP}) = Q_p \times 100/(Q_p + Q_{CP}) \tag{11}$$

$$SE_{HP} = p_{av}/36/f_{HP} \tag{12}$$

$$SE_{CP} = Q_{CP} \times \Delta p/36/f_{CP}/Q_p \tag{13}$$

$$SE_{total} = p_{av}/36/f_{HP} + Q_{CP} \times \Delta p/36/f_{CP}/Q_p \tag{14}$$

3. Modular BWRO-CCD NME*n* units design

The continuously staged flow and pressure boosted BWRO-CCD technology involves simple units with high modularity expressed by NMEn (n = 1–4), wherein n stands for the number of elements per pressure vessel and N for the number of pressure vessels per design. The flow and volume set points of operation of modular designs are N time those of a single module apparatus, and the performance characteristics are independent of the number of pressure vessels per design. The modular designs comprise pressure vessels with their inlets and outlets connected in parallel to the closed circuit, and therefore each module in the system operates autonomously independent of the others. The design of modular units should rely on good hydraulic practices to enable uniform and efficient flow distribution with minimum flow-induced pressure losses. Three typical modular deigns of 5ME4 (20–25 m^3/h, 480–600 m^3/d), 10ME4 (40–50 m^3/h, 960–1,200 m^3/d) and 20ME4 (80–100 m^3/h, 1,920–2,400 m^3/d), are displayed in Figs. 2–4, respectively, with their

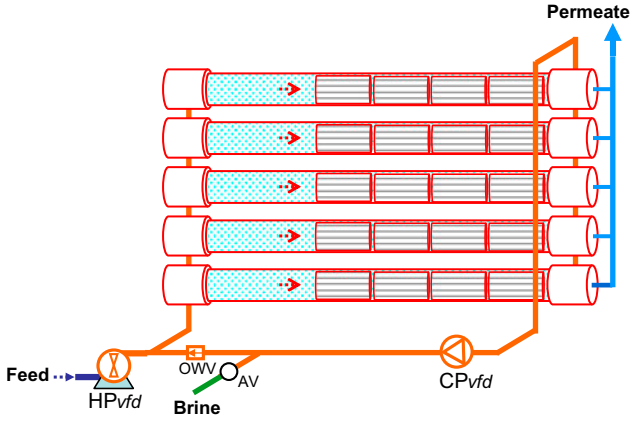

Fig. 2. Illustration of a compact modular BWRO-CCD 5ME4 unit design with 5 vertically stacked pressure vessels for permeate production of 20–25 m^3/h (480–600 m^3/d).

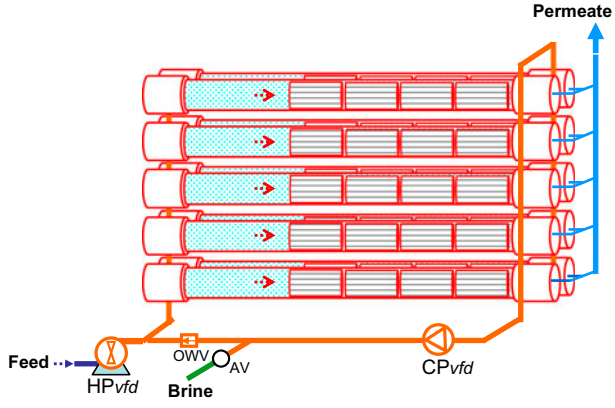

Fig. 3. Illustration of a compact modular BWRO-CCD 10ME4 unit design with flow distribution at inlets and outlets of modules through manifolds for permeate production of 40–50 m^3/h (960–1,200 m^3/d).

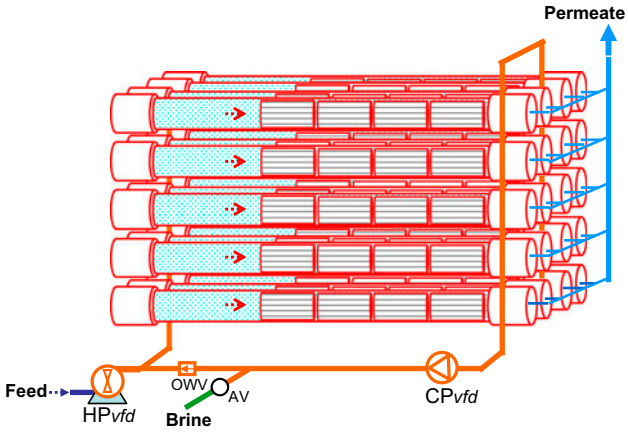

Fig. 4. Illustration of a compact modular BWRO-CCD 20ME4 unit design with inlets and outlets flow distribution through manifolds to a twine-coupled pressure vessels configuration for permeate production of 80–100 m^3/h (1,920–2,400 m^3/d).

production ranges in parentheses reflecting a maximum selected flux of 27 lmh. The design in Fig. 2 comprises five parallel vertically stacked pressure vessels, whereas in Fig. 3 flow distribution at the inlets and outlets of modules takes place through manifolds, and in Fig. 4 the design also incorporates a configuration of horizontally coupled pressure vessels. The recovery of the units under review is confined only by the compositions of the feed source and the pressure rating limitations of components. The units under review ordinarily require free volume in pressure vessels equivalent to free space of one element if operated in the recovery range of 85–88% in order to allow for a preferred sequential period (≥10 min) and such a feature is not required when recovery is ≥89%. The modular design of the units under review can be expanded in height and/or width as long as the inlets and outlet of the individual pressure vessels are connected in parallel to the principle closed circuit.

4. Theoretical model analysis of single-sequence BWRO-CCD ME4 unit operation

The performance of BWRO-CCD units can be derived by theoretical model analysis at the level of an

Table 1
Theoretic sequence model simulation of a BWRO-CCD ME4 (E = ESPA2 MAX) module with feed of 2,500 ppm NaCl under fixed flow and variable pressure conditions at 25 lmh with the specified operational set-points of PFD [Q_{HP} = 5.10 m^3/h; Q_P = 1.28 m^3/h and MR = 25%] and CCD [Q_{HP} = Q_P = 4.08 m^3/h; Q_{CP} = 6.12 m^3/h; MR = 40%] in a closed circuit volume of 76.7 liters using a pressure vessel (8″) 430 cm long without any spacer(s) at 25°C and assuming 75% efficiency of both pumps

Test Conditions		Unit Design		PFD		CCD		General Information	
40.8	m^2/Element	1	Modules	0.250	% NaCl	0.33	% Initial feed	0.0694	av-MR/Element-PFD
45.4	m^3/day	4	Elements/Module	25	% increased HP flow	25.0	lmh Flux	0.1199	av-MR/Element-CCD
1,500	ppm NaCl	430	cm long PV	5.10	m^3/h Feed	40	% Module Recovery	1.066	av-pf - PFD
10.5	bar Applied Pressure	20	cm diameter PV	25	% Recovery	1.14	bar Δp	1.1167	av-pf - CCD
15	% Recovery	2	% added conduits	0.41	bar Δp	4.08	m^3/h Permeate (=Q_{HP})		
25	°C	15	liter per element	1.28	m^3/h Permeate	6.12	m^3/h Qcp	PUMPS	
99.6	% Salt Rejection	76.5	liter per module	3.83	m^3/h Brine	0.75	min/cycle CCD	0.75	HP Eff.
9.285	bar NDP			0.33	% Brine	0.051	m3/CCD-Cycle	0.75	CP Eff.
46.36	l/m^2/h Flux			7.8	lmh flux				
4.416	l/m^2/h/bar -A			1.20032	min/step PDF			TEMPERATURE	
0.146	l/m^2/h - B			0.02551	m^3/step Permeate			25	°C
8.00	π(bar)/C(%)-assumed			4.3	bar Applied Pressure			1.000	TCF

ME4 Module Data				Separate CCD Cycles & PFD Step						Combined Sequence (CCD Cycles & PFD Step)						PERMEATE			SLOPE
		Inlet	Outlet	Time	p_{appl}	HP	CP	HP+CP	per Step	Time	Permeate - m3		REC	Energy		mean	Step	mean	Δπ/ΔREC
Mode	Step	%	%	min	bar	kW	kW	kW	kWh/m3	Σmin	Step	Σm3	%	ΣkWh	kWh/m3	m3/h	ppm	ppm	bar/%
PFD	**0**	**0.25**	**0.33**	**1.20**	**4.3**	**0.813**	**0.000**	**0.813**	**0.638**	**1.2**	**0.026**	**0.026**	**25.0**	**0.016**	**0.638**	**1.28**	**58**	**58**	**0.027**
CCD	1	0.33	0.56	0.75	9.8	1.479	0.257	1.736	0.425	2.0	0.051	0.077	50.0	0.038	0.496	2.35	29	39	0.07
CCD	2	0.43	0.72	1.50	10.9	1.640	0.257	1.897	0.465	2.7	0.051	0.128	62.5	0.062	0.484	2.83	38	38	0.18
CCD	3	0.53	0.89	2.25	11.9	1.801	0.257	2.058	0.504	3.5	0.051	0.179	70.0	0.087	0.490	3.10	46	40	0.38
CCD	4	0.63	1.06	3.00	13.0	1.962	0.257	2.219	0.544	4.2	0.051	0.230	75.0	0.115	0.502	3.28	55	44	0.68
CCD	5	0.73	1.22	3.75	14.1	2.123	0.257	2.381	0.583	5.0	0.051	0.281	78.6	0.145	0.517	3.40	64	47	1.10
CCD	6	0.83	1.39	4.50	15.1	2.285	0.257	2.542	0.623	5.7	0.051	0.332	81.3	0.177	0.533	3.49	72	51	1.66
CCD	7	0.93	1.56	5.25	16.2	2.446	0.257	2.703	0.662	6.5	0.051	0.383	83.3	0.211	0.550	3.56	81	55	2.39
CCD	8	1.03	1.72	6.00	17.3	2.607	0.257	2.864	0.702	7.2	0.051	0.434	85.0	0.246	0.568	3.61	90	59	3.31
CCD	9	1.13	1.89	6.75	18.3	2.768	0.257	3.025	0.742	8.0	0.051	0.485	86.4	0.284	0.586	3.66	98	63	4.43
CCD	10	1.23	2.06	7.50	19.4	2.929	0.257	3.187	0.781	8.7	0.051	0.536	87.5	0.324	0.605	3.69	107	67	5.79
CCD	11	1.33	2.22	8.25	20.5	3.090	0.257	3.348	0.821	9.5	0.051	0.587	88.5	0.366	0.624	3.72	116	72	7.40
CCD	12	1.43	2.39	9.00	21.5	3.252	0.257	3.509	0.860	10.2	0.051	0.638	89.3	0.410	0.643	3.75	124	76	9.28
CCD	13	1.53	2.56	9.75	22.6	3.413	0.257	3.670	0.900	11.0	0.051	0.689	90.0	0.456	0.662	3.77	133	80	11.45
CCD	14	1.63	2.72	10.50	23.7	3.574	0.257	3.831	0.939	11.7	0.051	0.740	90.6	0.504	0.681	3.79	142	84	13.94
1	2	3	4	5	6	7	8	9	10	11	12	13	14	15	16	17	18	19	20

isolated sequence as well as a continuous consecutive sequential process, and this is illustrated in Table 1 for an apparatus of the ME4 (E = ESPA2-MAX) design as in Fig. 1 with feed source of 2,500 NaCl of π = 2.0 bar at 25°C which is the equivalent of common brackish water sources in the salinity range of 2,700–3,000 ppm. It should be pointed that conventional computer design programs of membrane manufacturers are unfit for complete BWRO-CCD simulations since this technology is based on different operational principles compared with conventional techniques. But, isolated steps in the BWRO-CCD process can be ascertained with the aid of conventional design programs, which can also be found useful to evaluate certain empirical factors of direct specificity to the type of membrane element and its internal design, such as z in Eq. (6) for $\Delta\pi$ and k in Eq. (4) for pf_{av}. The simulation data presented in Table 1 pertains to a single sequence with its PFD step and CCD cycles.

The entire data in Table 1 originates from theory using conventional RO and power equations with explanation provided below according to the labeled columns in the bottom of the table. The database for the simulations is listed at the top of the table. The mode of the sequence is defined in column 1 and the step in column 2 wherein 0 stands for PFD and the numbers for CCD cycles. The module inlet and outlet % concentrations are outlined in columns 3 and 4, respectively, and the duration (minutes) of PFD and cumulative CCD cycles are provided in column 5. The applied pressure (bar) during PFD and the variable applied pressures during CCD are derived by Eq. (2) and provided in column 6. The power (kW) for HP in column 7 is derived from Eq. (15) and for CP in column 8 from Eq. (16) and the sum of both pumps is listed in column 9.

$$P_{HP}(\text{kW}) = p_{appl} \times Q_{HP}/36/f_{HP} \quad (15)$$

$$P_{CP}(\text{kW}) = \Delta p \times Q_{CP}/36/f_{CP} \quad (16)$$

The specific energy (kWh/m^3) per PFD step or CCD cycle in column 10 is derived from the expression P (kW)/Q_p(m^3/h) for the PFD step and each of the CCD cycles. The combined (PFD + CCD) cumulative sequence time (min) is provided in column 11. The permeates produced volumes (m^3) during the PFD step and CCD cycles, which are provided in column 12; their sequential accumulations (Σm^3) in column 13, together with the fixed closed circuit intrinsic volume (V = 76.5 L), provide the sequential recovery data in column 14 according to Eq. (8) as expressed by $\Sigma V_p/(\Sigma V_p + V) \times 100$, wherein ΣV_p stands for the cumulative sequential permeate volume and V for the intrinsic closed circuit volume. The cumulative energy (ΣkWh) of HP and CP during the PFD step and CCD cycles of the sequential progression is provided in column 15 and this information together with the relevant cumulative permeate volumes in column 13 (Σm^3) gives the mean sequential specific energy terms in column 16 according to the expression ΣkWh/Σm^3. Additional information in Table 1 pertaining to permeates includes the mean sequential permeate production flow rate (m^3/h) during the PFD-CCD progression in column 17, permeates' TDS (ppm) per PFD step and CCD cycles in column 18, and their mean value in column 19. Permeate TDS (ppm) is derived by Eq. (3) using the average concentration polarization term (pf_{av}) derived by Eq. (4) (k = 0.4) and the and average module recovery per element term (Y_{av}) derived by Eq. (5). The k = 0.4 factor used in Eq. (4) was derived from the IMD-designed program for the ESPA2-MAX element in a module of four elements operated under same flow and flux conditions described in Table 1. The final column in Table 1 labeled 20 pertains to the SLOPE (bar/%) expressing osmotic pressure difference per recovery difference ($\Delta\pi/\Delta R$) during the sequential PFD step and CCD cycles. In simple terms, the SLOPE expresses the average osmotic pressure rise per each additional percent of recovery and manifests the pressure-boosting requirements of HP under the fixed flow and variable pressure conditions of the BWRO-CCD technology.

The results of the theoretical model simulations in Table 1 are displayed as followed: Fig. 5(A–C) describes the sequential applied pressure variations during CCD cycles (A), on time scale (B), and on recovery scale (C). Fig. 6(A–D) describe the sequential power variations during CCD cycles (A) and their effects on specific energy (B), and the same is also expressed on the recovery scale with respect to power (C) and specific energy (D). Fig. 7(A–B) describe the sequential SLOPE ($\Delta\pi/\Delta R$—bar/%) variations experienced during CCD cycles (A) as well as on the recovery scale (B). Fig. 8(A–B) describe the sequential salinity variations of permeates during CCD cycles (A) and on the recovery scale (B).

The theoretical model simulation results of the BWRO-CCD ME4 (E = ESPA2-MAX) unit in Table 1 reveal a sequential pressure-boosted process under fixed flow conditions of linear relationship to CCD cycles (Fig. 5 (A)) and time (Fig. 5(B)) and exponential relationship to recovery (Fig. 5(C)) with rapid pressure rise associated with increased recovery. The term "per step" used in Fig. 5 and hereinafter refers to a specific data point during the sequential progression and "mean" to an average, which also takes account of the preceding data points. The principle features in Fig. 5 of low PFD pressure and the diagonal pressure rise

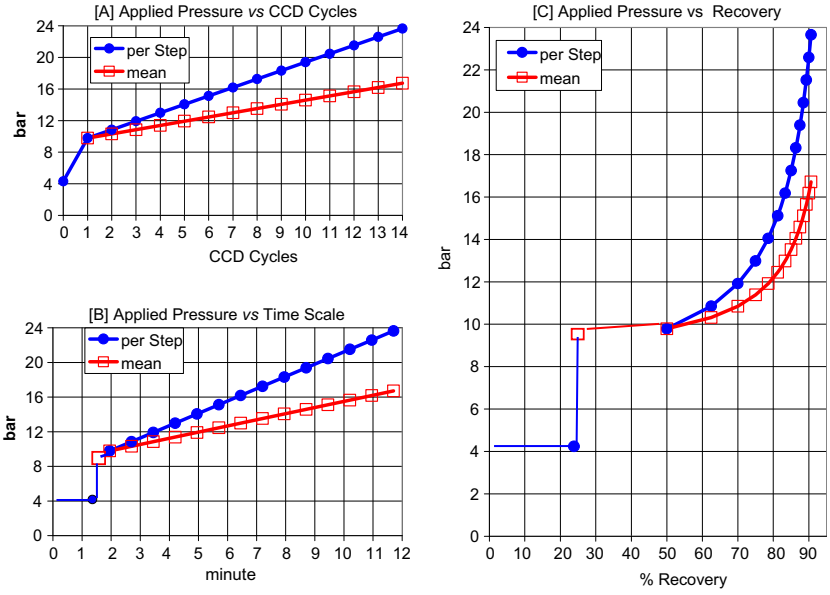

Fig. 5(A–C). Sequential applied pressure variations during CCD cycles (A) on time scale (B) and on recovery scale (C) according to the data furnished in Table 1.

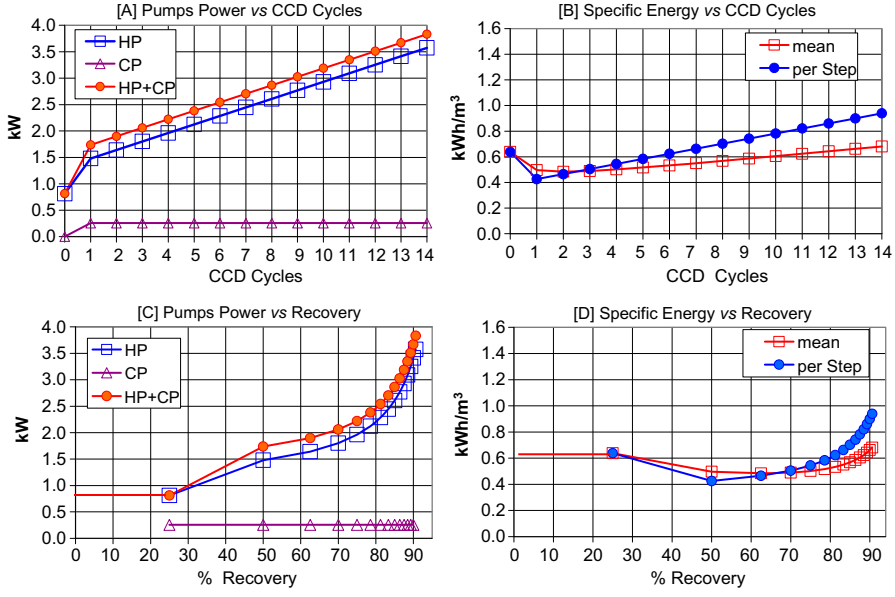

Fig. 6(A–D). Sequential power variations during CCD cycles (A) and their effects on specific energy (B) and the same variations also exemplified on the recovery scale with respect to power (C) and specific energy (D) according to the data furnished in Table 1.

during CCD cycles do suggest an energetically efficient process of low specific energy and small energy loss during the brief brine rejection intervals. The sequential pressure variations under fixed flow conditions displayed in Fig. 5 bear some resemblance to conventional BWRO of staged flow design configuration with inter-stage pressure boosters and such effects in CCD are created by simple means without the need of staged pressure vessels and/or booster pumps.

The variable applied pressure characteristics of BWRO-CCD displayed in Fig. 5 most obviously dictate the power and energy behavior of the system

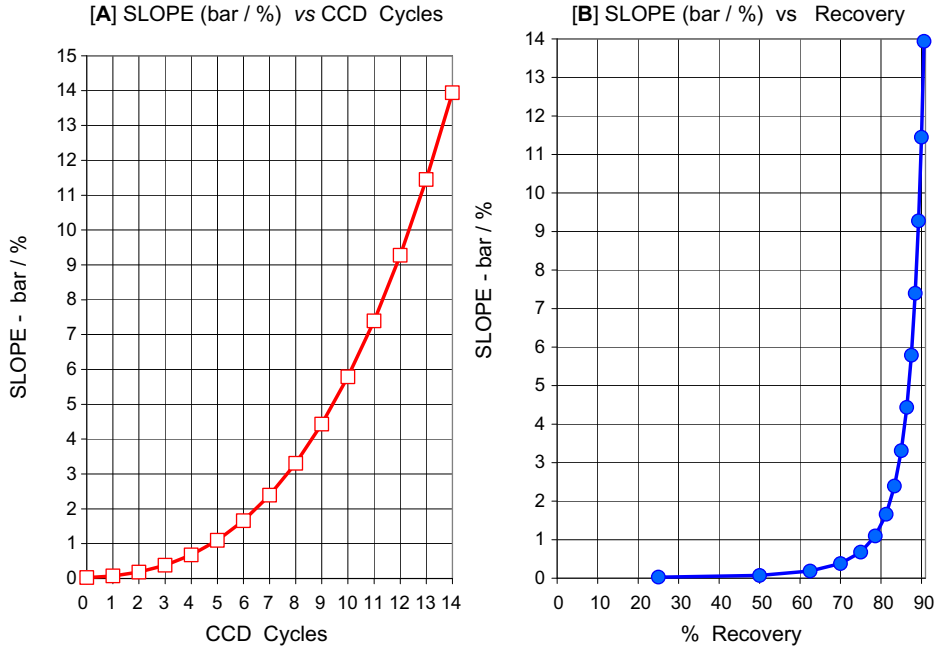

Fig. 7(A–B). : Slope ($\Delta\pi/\Delta R$—bar/%) sequential variations experienced during CCD cycles (A) and on the recovery scale (B) according to the data furnished in Table 1.

revealed in Fig. 6 with linear power demand (A) and specific energy (B) as functions of CCD cycles and exponential relationship of the respective terms to recovery ((C) and (D)). The rather sharp rise of power demand (2.542–3.670 kW) in the recovery range 81.3–90.0% revealed in Table 1 and in

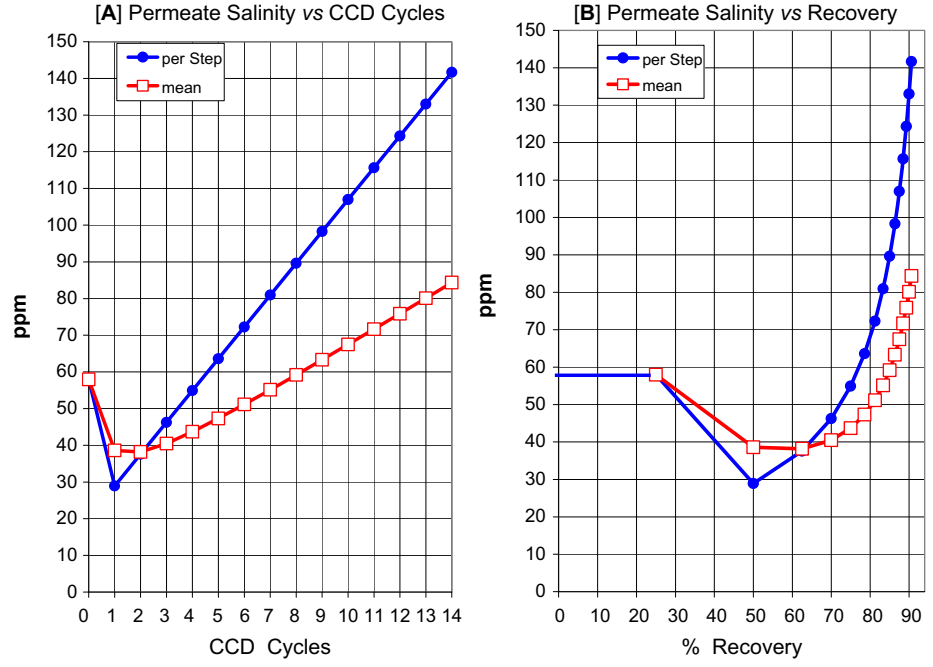

Fig. 8(A–B). Sequential salinity variations of permeates during CCD cycles (A) and on the recovery scale (B) according to the data furnished in Table 1.

Fig. 6(C) is accompanied by a rather modest rise in the mean specific energy (0.533–0.662 kWh/m^3) displayed in Fig. 6(D), and this noteworthy comparison is just another illustration of the high energy efficiency of the BWRO-CCD process even at high recovery. The rapidly rising osmotic pressure of recycled concentrates at high recovery explains the exponential rise of power demands by HP in order to sustain adequate applied pressure for fixed flow production of permeates and this high recovery power constrain of pressure boosting by HP-vfd in CCD is manifested amongst others by the so-called SLOPE of $\Delta\pi/\Delta R$ (bar/%) in column 20 of Table 1 as well as in Fig. 7(A) as a function of CCD cycles and in Fig. 7(B) as function of recovery. The pressure boosting of HP-vfd is confined to a certain maximum SLOPE and this limitation constitutes an important criteria for the selection of suitable HP (vfd) for a specific BWRO-CCD application.

The data in Table 1 considered hereinabove pertain to a single-sequence (PFD + CCD) performance of a defined ME4 unit under fixed flow and variable pressure conditions with the intent to show the expected performance by limiting applied pressure of operation to a selected maximum which manifests the desired recovery by means of a defined set point on the control board of the unit. For instance, the selection of 17.3 bar as the maximum applied pressure set point in the context of the BWRO-CCD ME4 unit described in Table 1 implies the attainment of 85% recovery by 7.2-min-long sequences of eight CCD cycles with mean specific energy of 0.568 kWh/m^3, mean permeate production of 3.61 m^3/h, mean permeate salinity of 59 ppm, and SLOPE of 3.31 bar/%. The selection of 22.6 bar as the maximum applied pressure set point in the unit under review implies the attainment of 90% recovery by 11.0-min-long sequences of 13 CCD cycles with mean specific energy of 0.662 kWh/m^3, mean permeate production of 3.77 m^3/h, mean permeate salinity of 80 ppm, and SLOPE of 11.45 bar/%. A cut-off of the pressure boosting of HP-vfd by an assumed SLOPE ≤ 15.0 bar/% limitation should enable the said unit to operate with up to 91% recovery with a maximum applied pressure around 25 bar.

5. BWRO-CCD ME4 model theoretical consecutive sequential simulations

The theoretical model simulations in Table 1 pertain to a single BWRO-CCD sequence comprising a PFD step and up to 14 CCD cycles with maximum recovery of 90.6%. In order to enable the unit defined in Table 1 to operate continuously by a consecutive sequential process, it is necessary to define the set point of maximum applied pressure which triggers the CCD-PFD shift during the said process. The PFD-CCD shift during this process is triggered by a volume-meter monitor when the replaced volume of brine by fresh feed matches the intrinsic closed circuit volume set point. For instance, 90% recovery according to the database furnished in Table 1 is attained with 13 CCD cycles at an applied pressure of 22.6 bar, which should be selected as maximum pressure set point if such a recovery is desired. Sequence duration of 11.0 min associated according to Table 1 with 90% recovery at 22.6 bar maximum applied pressure implies an average of 5.45 sequences per hour. Variations and/or changes of parameters over a 60-min span during the continuous consecutive sequential BWRO-CCD operation at 90% recovery according to the data in Table 1 are illustrated in Fig. 9(A-B) for flow (A) and flux (B); in Fig. 10(A–B) for applied pressure (A) and power (B); in Fig. 11(A–B) for specific energy (A) and SLOPE (B); in Fig. 12(A–B) for the salinity of recycled concentrates (A) and permeates (B); and in Fig. 13(A–B) for MR and average element recovery (A) and beta as well as Δp (B).

The time scale performance illustrations in Figs. 9–13 cover a 60-min span of almost 5.45 sequences, each of 11-min duration, with respective parameters consistently repeated. During 89% of the time the system performs CCD and 11% of the time PFD and the CCD principle parameters of pressure, power, concentrations, and SLOPE are progressively increased from minimum to maximum with overall process expressed by their mean values. The fixed flow (Fig. 9) and variable pressure (Fig. 10(A)) CCD operation is noteworthy in particular since illustrates the staged flow and pressure-boosting characteristics of the process whereby power consumption along a diagonal (Fig. 10(B)) enables exceptionally low specific energy without the need of energy recovery – a process unattainable by any other technique. The pressure boosting as function of recovery is also manifested by the bar/% SLOPE in Fig. 11(B) which reveals the range 0.07–11.45 between the start and end of CCD at 90% recovery. Concentration variations on time scale of recycled concentrates (Fig. 12(A)) illustrate the dilution effect by the mixing of fresh feed with recycled concentrates at the inlet to module and the permeate concentrations in Fig. 12(B) are said for CCD flux of 25 lmh and reflect the rejection characteristics (99.6%) of the selected element (ESPA2-MAX) in the simulation. Despite the very large and frequent variations of concentrations and pressures revealed on the time scale of operation, the PFD and CCD membranes'

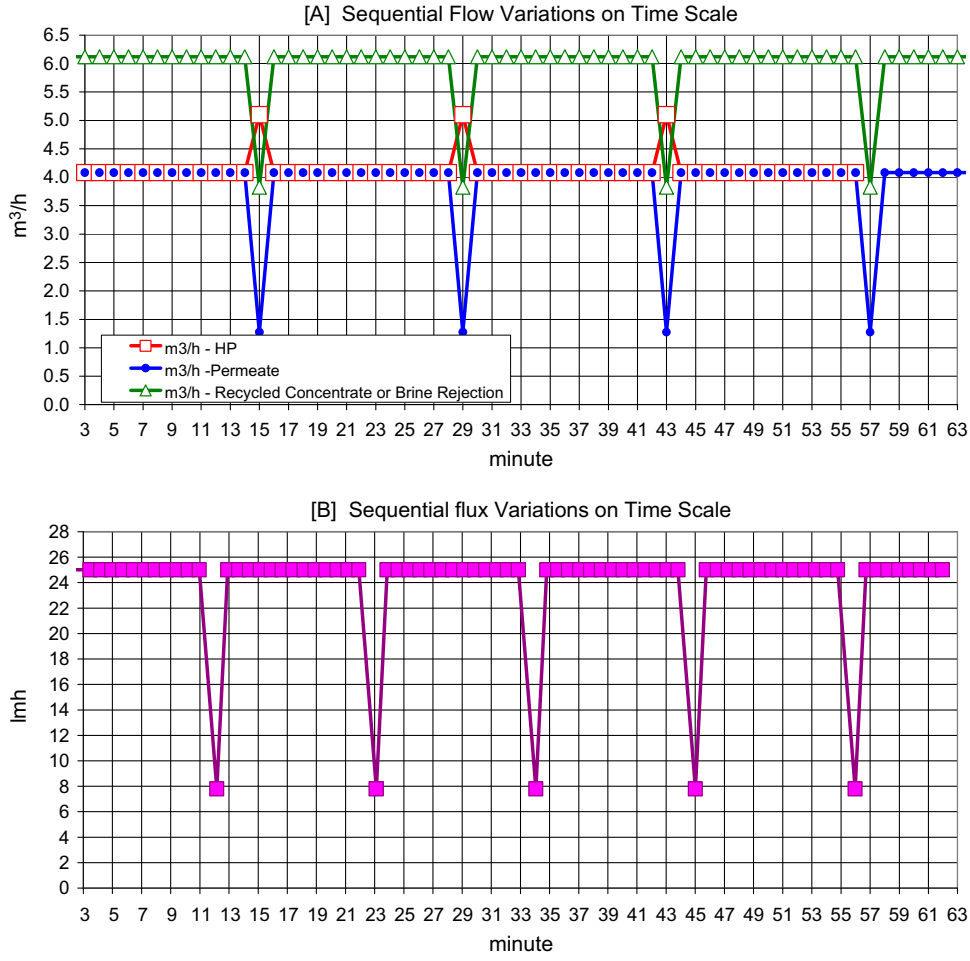

Fig. 9(A–B). Continuous consecutive sequential variations of flow (A) and flux (B) during the 90% recovery of NaCl 2,500 ppm under the conditions specified in Table 1.

parameters remain essentially unchanged as evident by the MR and the average element recovery in Fig. 13(A) as well as by beta in Fig. 13(B).

6. Effects of database changes on BWRO-CCD ME4 model performance

The principle control set points of the BWRO-CCD operation include the flow rate of HP during PFD, the flow rate of HP during CCD, the flow rate of CP during CCD, and the maximum pressure CCD limit. Change of set points may take place "on line" and the effects created by such a change when made one at time can be ascertained in the context of the theoretical model database in Table 1 at the sequential and/or the consecutive sequential levels. Apart from set points, the database also contains noteworthy information concerning structural features (e.g. pressure vessels, elements, etc.) and feed, which shall be considered next in the context of theoretical model performance.

6.1. MR change effects on performance

Change of CCD MR (35%→40%→45%→50%) in Table 1, leaving all other parameters unchanged, implies change of cross flow (Q_{CP}) without change of flux. According to Eq. (11), increased MR is associated with decreased cross flow and increased time period per CCD cycle (time/cycle = V/Q_{CP}), which is also manifested by longer sequences of higher exemplified by Fig. 14 in relationship to CCD cycles as function of sequence time (A) and recovery (B). In simple terms, sequences of same number of CCD cycles with increased MR become longer and lead to higher recovery. The aforementioned statement implies the ability to dictate by MR selection the number of CCD cycles required to reach a desired

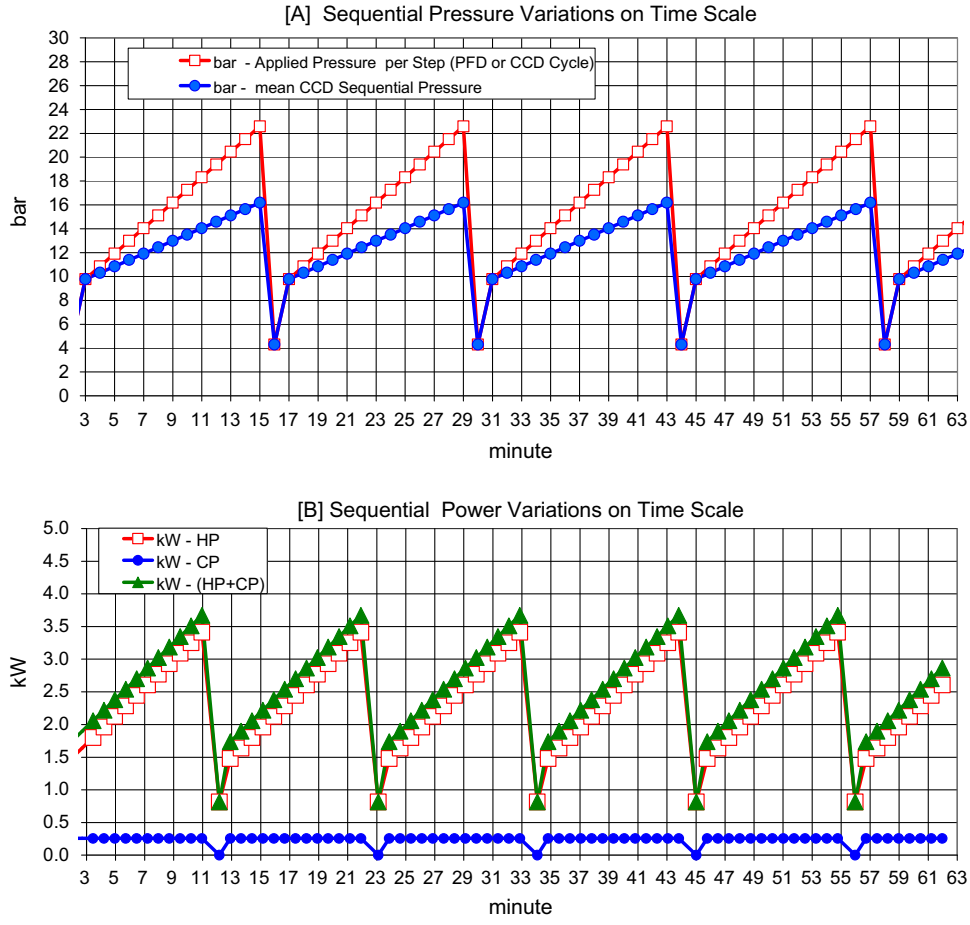

Fig. 10(A–B). Continuous consecutive sequential variations of pressure (A) and power (B) during the 90% recovery of NaCl 2,500 ppm under the conditions specified in Table 1.

recovery. For instance, focusing on sequences with 10 CCD cycles in Fig. 14(A) reveals sequence duration as function of MR (in brackets) of 7.3(35%), 8.7 (40%), 10.4(45%), and 12.5(50%) minute with the respective recoveries of 85.1(35%), 87.5(40%), 89.5 (45%), and 91.2(50%) revealed in Fig 14(B). Cross flow variations by MR selection without change of flux create only minor effects of specific energy and/or quality of permeates which are determined primarily by flux. Minor effects with respect to specific energy arise from the cross flow contribution to the specific energy of CP which is a minor constituent in the overall specific energy of the process. The minor MR effects on salt rejection arise according to Eq. (3) from the concentration polarization term (pf_{av}) in Eq. (4), wherein Y_{av} stands for the average element recovery term expressed by Eq. (5) which takes account of MR. The information in Table 1 for MR = 40%; 90.6% recovery; 14 CCD cycles; and 11.7 min sequence duration complies with the data presented in Fig. 14.

6.2. Flux change effects on performance

Change of flux in the model simulation database under review in Table 1 with retention of MR = 40% takes place by entering a new desired flux value (e.g. 17.5; .20.0; 22.5; and 27.5 lmh) instead of the registered flux value (25 lmh), and this automatically leads to adjustments of both CCD flow rates of HP (Q_f) and CP (Q_{CP}) to meet the desired MR in compliance with Eq. (11). CCD flux variations with retention of MR should in theory effect the sequential period, specific energy, and concentration of permeate without effecting the relationship between CCD cycles and recovery which depends on MR. The effects of aforementioned flux variations (17.5–27.5 lmh) with fixed MR = 40% are illustrated in reference to the CCD flow rates of HP (Q_f) and

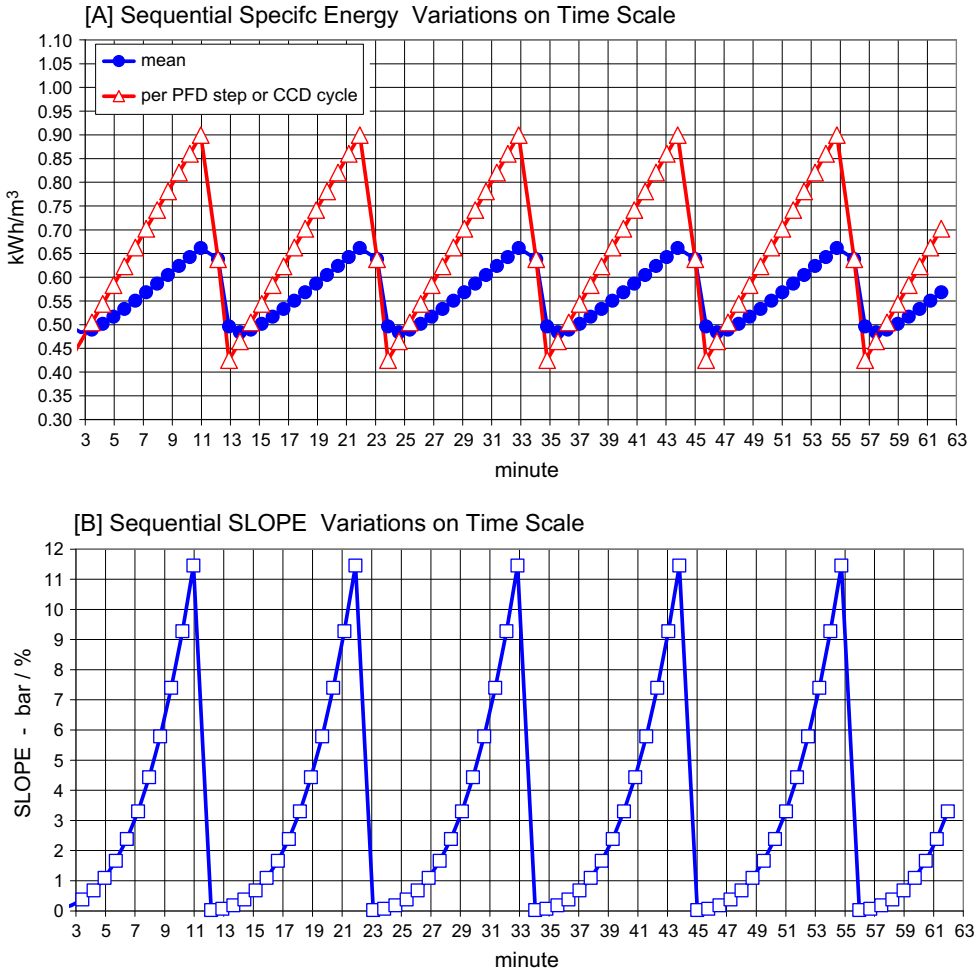

Fig. 11(A–B). Continuous consecutive sequential variations of specific energy (A) and SLOPE (B) during the 90% recovery of NaCl 2,500 ppm under the conditions specified in Table 1.

CP (Q_{CP}) in Fig. 15(A), and on the recovery scale of sequence duration in Fig. 15(B), specific energy in Fig. 16(A), and mean permeate TDS in Fig. 16(B). Increased flux should effect shorter sequence periods, increased specific energy, and declined mean TDS of permeates. The slight decline of specific energy in the 70–79% range in Fig. 16(A) manifests the declined relative energy contribution of PFD to average specific energy.

6.3. Maximum CCD pressure change effects on performance

Recovery in BWRO-CCD depends only on the maximum CCD sequential pressure selection irrespective MR and/or flow and/or flux. The maximum CCD sequential pressure set point corresponds to the salinity of the recycled concentrate at the desired recovery level of the system. The desired recovery can be selected with any desire flux and/or flow and/or MR with an infinite number of available combinations, and this exemplifies the extraordinary flexibility of the CCD technology with higher maximum pressure selection concomitant with higher recovery and vice versa. In the context of the theoretical BWRO-CCD model of 2,500 ppm NaCl with MR = 40% under the conditions specified in Table 1, the relationships between CCD maximum pressure selection and recovery are illustrated in Fig. 17 and exemplified with a 17.3 bar maximum CCD pressure selection under which conditions desalination is achieved with 85% recovery and mean specific energy of 0.568 kWh/m^3 yielding permeates of 59 ppm mean TDS. Increased maximum pressure set point implies permeates production of higher salinity with greater specific energy and vice

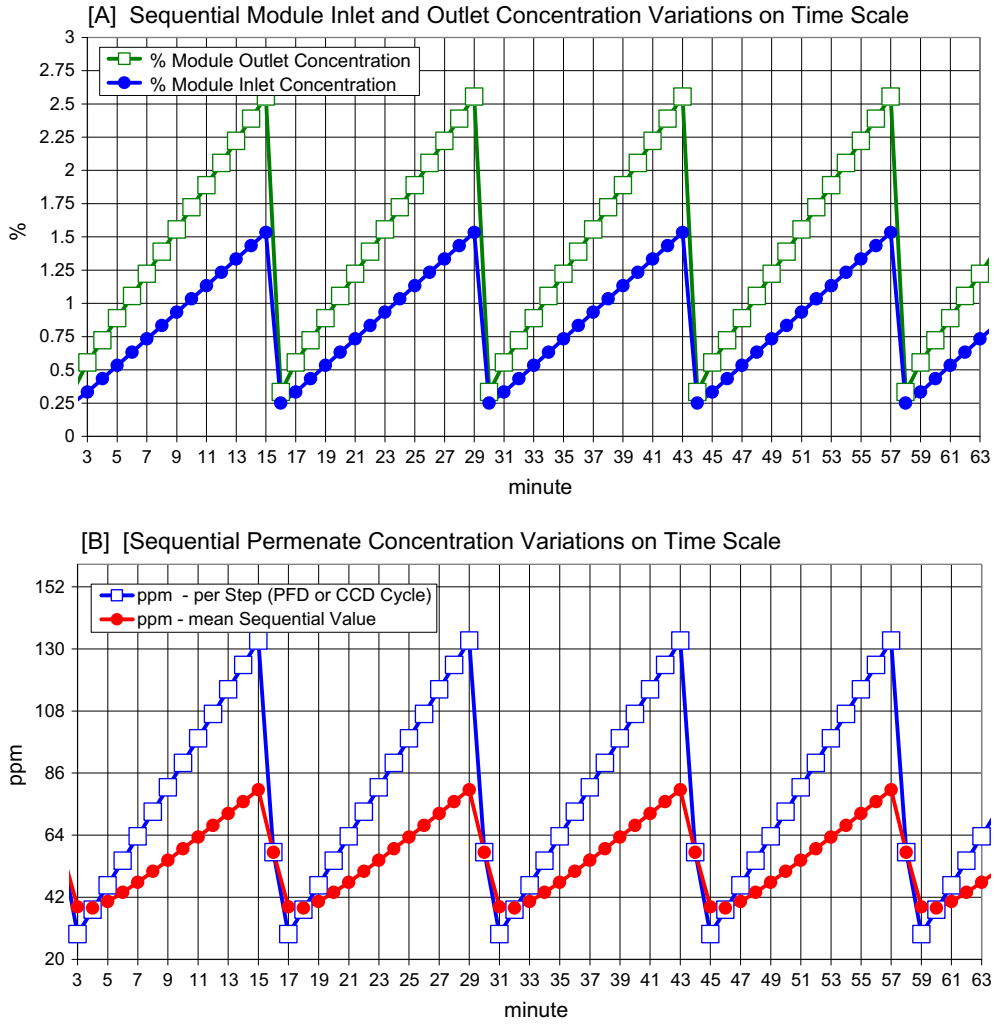

Fig. 12(A–B). Continuous consecutive sequential variations of concentrations of recycled concentrates (A) and permeates (B) during the 90% recovery of NaCl 2,500 ppm under the conditions specified in Table 1.

versa. Fore example, maximum CCD pressure selection of 22.6 bar in the system under review allows 90% recovery with mean specific energy of 0.692 kWh/m^3 and yields permeates of 80 ppm mean TDS.

6.4. PFD set points effects on model performance

The information connected to the PFD step in the database displayed in Table 1 relates to the salinity of the feed source, the desired % increase in the feed flow of HP experienced during PFD compared with CCD, and the desired recovery during this step of the consecutive sequential process. The actual set points during this step in the process include the feed flow rate (Q_{PFD}) by HP and the desired recovery or permeate flow instead. The referred set points dictate the pressure and duration of the PFD step with a faster brine replacement by fresh feed induced by increased Q_{PFD} and decreased recovery and vice versa. The pressure during the PFD step will depend primarily on the choice Q_{PFD} and recovery or flux and recovery. A minor set point during PFD relates to the volume of replaced brine by fresh feed, and while this volume is in theory the fixed intrinsic free volume of the closed circuit some small adjustments may be warranted in order to account for some mixing at the interface of fresh feed and rejected brine.

6.5. Intrinsic closed circuit volume effects on model performance

The intrinsic volume of the closed circuit is determined by the diameter and length of the pressure vessel (PV) and the number of elements per PV. The

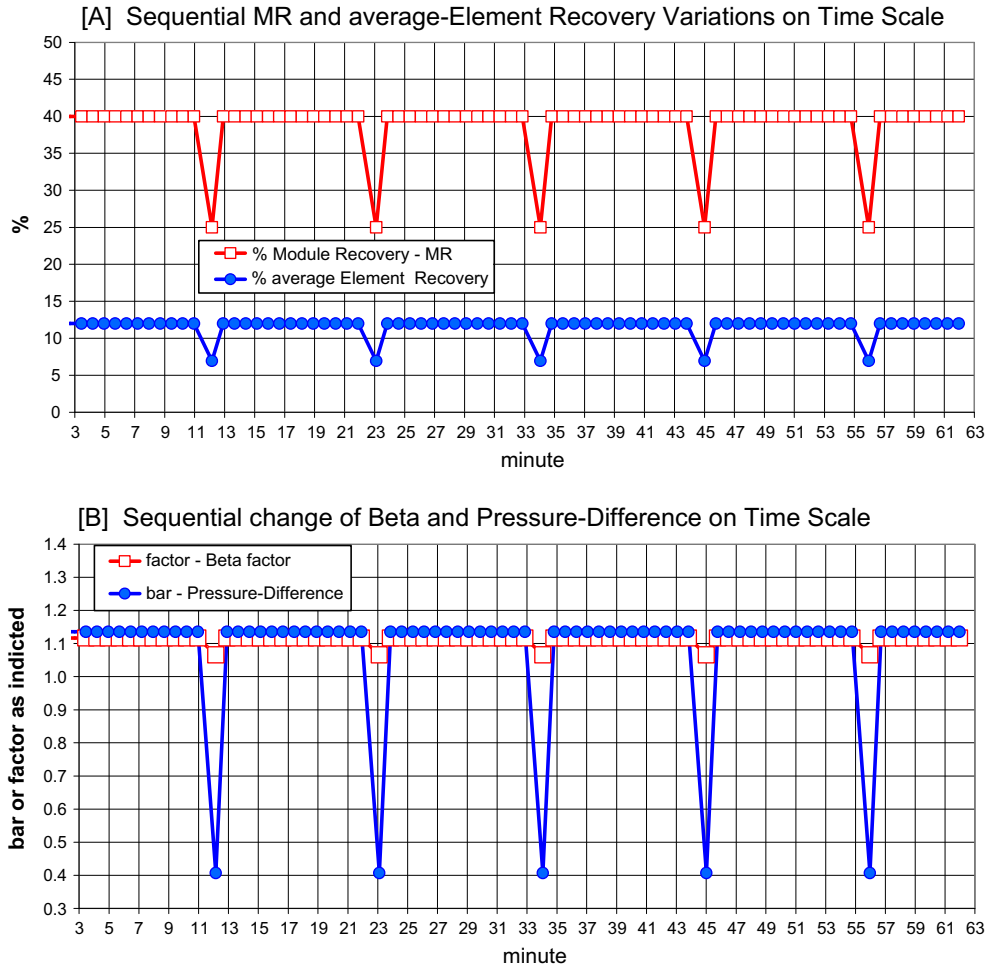

Fig. 13(A–B). Continuous consecutive sequential change of MR and average element recovery (A) as well as of beta factor and Δp (B) during the 90% recovery of NaCl 2,500 ppm under the conditions specified in Table 1.

data in Table 1 pertain to a design comprising four elements PV of 8´´diameter and 430 cm length of 76.5 L intrinsic closed circuit volume and its association with a sequence of 90% recovery by 13 CCD cycles over 11.0 min duration. The volume of the closed circuit is determined at the design stage and in reference to modules of the ME4 configuration the intrinsic free volume is determined by the length of the PV and the number of elements and spacers inside. For instance, intrinsic closed circuit volumes of ME4 modules in pressure vessels which are 430; 530; 630; 730, and 830 cm long are 76.5; 108.5; 140.6; 172.6, and 204.6 L, respectively, and the respective number of spacers of a common element dimensions required for their installation are 0, 1, 2, 3, and 4. A change of PV length in the database section of Table 1 without changing any of the other parameters in the table should effect a linear change of intrinsic closed circuit volume manifested by change of sequence duration according to Eq. (10), and the relationship between closed circuit volume and sequence duration in the system under review at 90% recovery is revealed in Fig. 18. The preferred sequence duration of BWRO-CCD systems is in the range of 10–15 min during which ~90% is associated with CCD cycles. The aforementioned statement describes the design tools which enable the attainment of the desired sequence schedule at the intended working conditions of BWRO-CCD units. Emphasis should be made again to the fact that intrinsic volume selection at the design stage only effects the sequence duration and not any of the operational parameters of the system variation of parameters revealed over a time span of 60 min in Figs. 9–13 for 90% recovery of NaCl 2,500 ppm under the conditions specified in Table 1 for 76.5 L intrinsic volume will be the same for any other intrinsic volume selection except for

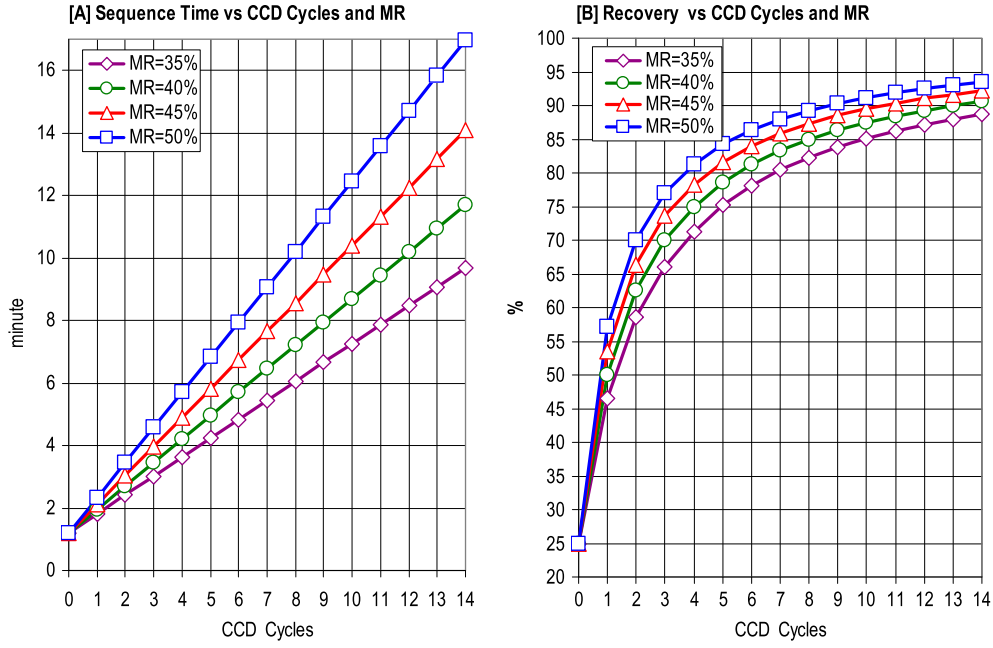

Fig. 14(A–B). Sequence time (A) and recovery (B) variations as function of CCD cycles for different MR in the BWRO-CCD model simulations of 2,500 ppm NaCl under the conditions specified in Table 1.

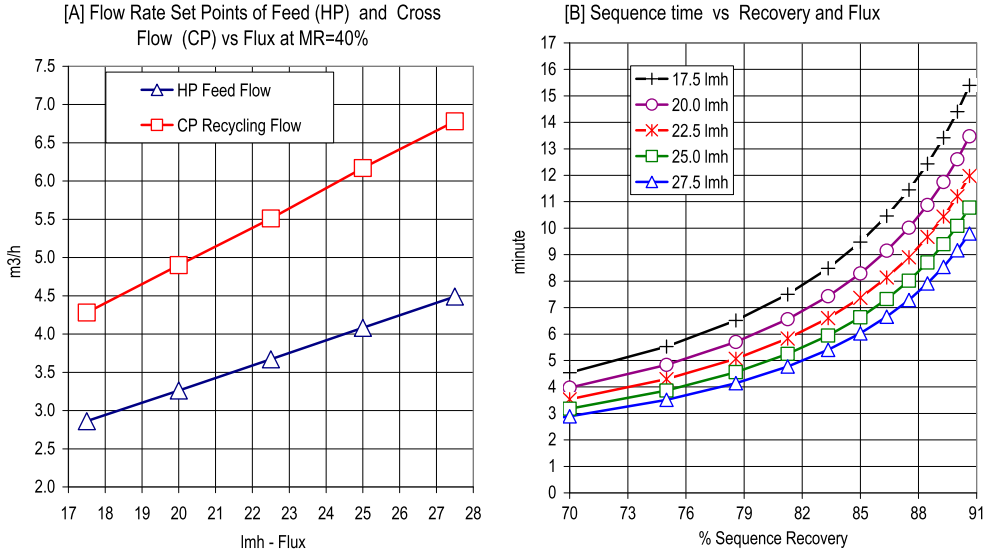

Fig. 15(A–B). CCD flow rates of HP (Q_f) and CP (Q_{CP}) *vs* flux (A) and sequence period *vs* recovery and flux (B) in the BWRO-CCD model simulations of 2,500 ppm NaCl with MR = 40% under the conditions specified in Table 1.

sequence duration as illustrated in Fig. 18. In simple terms, increased intrinsic volume will cause decreased number of sequences over the 60-min span, exemplified in Figs. 9–13, without any change in the values of parameters.

6.6. Feed salinity effects on model performance

Most conventional BWRO desalination applications are commonly practiced in the feed salinity range of 500–6,000 ppm with 75–90% recovery utilizing flow staged pressure vessels and auxiliary inter-staged boosters if subsequent stages involve high concen-

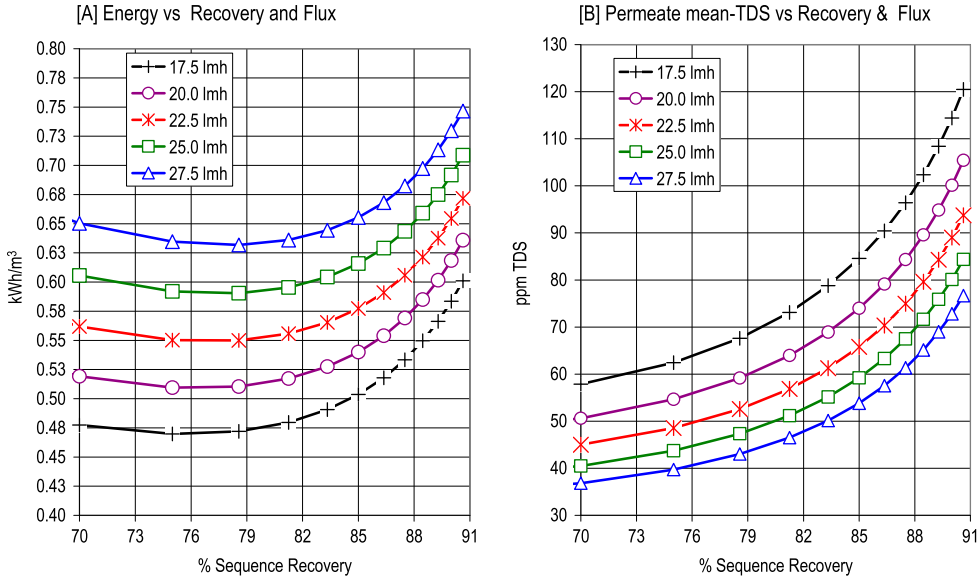

Fig. 16(A–B). Specific energy (A) and mean permeate TDS (B) variations as function of recovery in the BWRO-CCD model simulations of 2,500 ppm NaCl with MR = 40% under the conditions specified in Table 1.

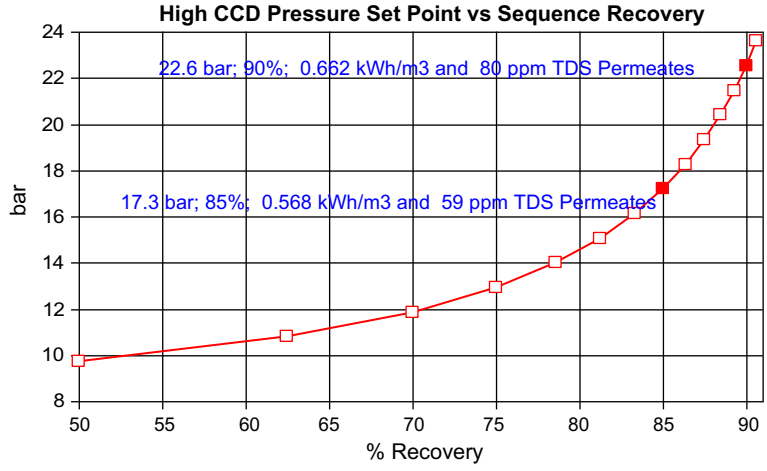

Fig. 17. Maximum CCD pressure as function of recovery in the BWRO-CCD model simulation of 2,500 ppm NaCl with MR = 40% under the conditions specified in Table 1.

trates. Accordingly, it should be of clear interest for a comparative purpose to ascertain the BWRO-CCD ME4 model performance in the same specified range of feed salinity and recovery, a subject matter considered next. The feed salinity effects in the context of the theoretical model analysis are evaluated by applying the feed salinity values of 500, 1,500, 3,000, 4,500, and 6,000 ppm NaCl in the database of Table 1 without changing any of the parameters except the length of the pressure vessel (530 instead of 430 cm) to allow for somewhat longer sequence periods due to the increased intrinsic closed circuit volume (108.5 instead of 76.5 L). Increased intrinsic volume does not change any of the performance characteristics of the system (see Section 6.4) and at the same time allows for reasonably longer sequences even when the maximum attainable recovery is below 90%. The salinity range of 500–6,000 ppm NaCl corresponds to the osmotic pressure of common brackish water sources in the salinity range of 550–7,000 ppm.

The results of the model simulations according to the database in Table 1 with NaCl concentrations of 500–6,000 ppm are revealed with respect to sequence period and recovery in relationship to CCD cycles in

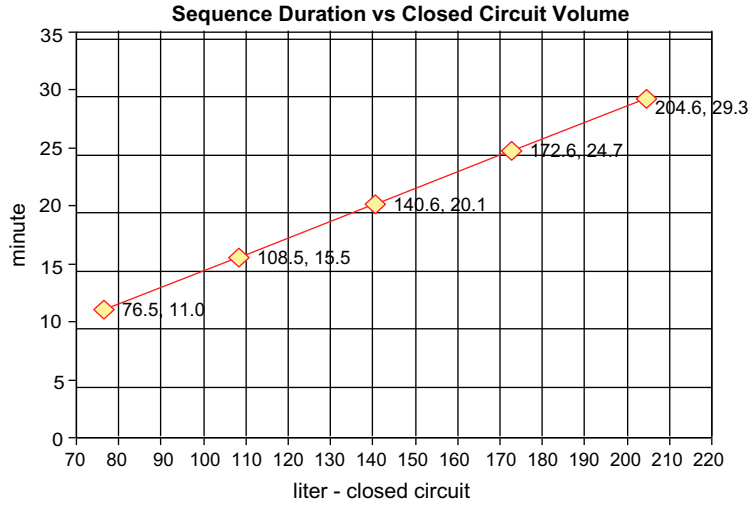

Fig. 18. Sequence time at 90% recovery as function of intrinsic closed circuit volume in the BWRO-CCD model simulation of 2,500 ppm NaCl with MR = 40% under the conditions specified in Table 1.

Fig. 19; applied CCD pressure as function of feed salinity in relationships to CCD cycles in Fig. 20(A) and recovery in Fig. 20(B); specific energy as function of feed salinity in relationships to CCD cycles in Fig. 21(A) and recovery in Fig. 21(B); mean permeate TDS as function of feed salinity in relationships to CCD cycles in Fig. 22(A) and recovery in Fig. 22(B); and SLOPE ($\Delta\pi/\Delta$Recover —bar/%) as function of feed salinity in relationships to CCD cycles in Fig. 23(A) and recovery in Fig. 23(B).

The results in Fig. 19 confirm that recovery, CCD cycles, and sequence period are independent of feed salinity as evident by the same performance profile irrespective of feed salinity. The applied pressures revealed in Fig. 20 show the dependence on feed salinity and sequence progression which is greatly enhanced with increased feed salinity. Common pressure vessels for BWRO applications are of 300 psi (~20.4 bar) and 450 psi (~30.7 bar) pressure ratings, and therefore confined to maximum recovery in the range of 82 → 87.5% with NaCl feed in the respective range of 6,000 → 4,500 ppm. Applied pressure during CCD cycles proceeds along a diagonal by an energy-saving mode not possible by any other existing

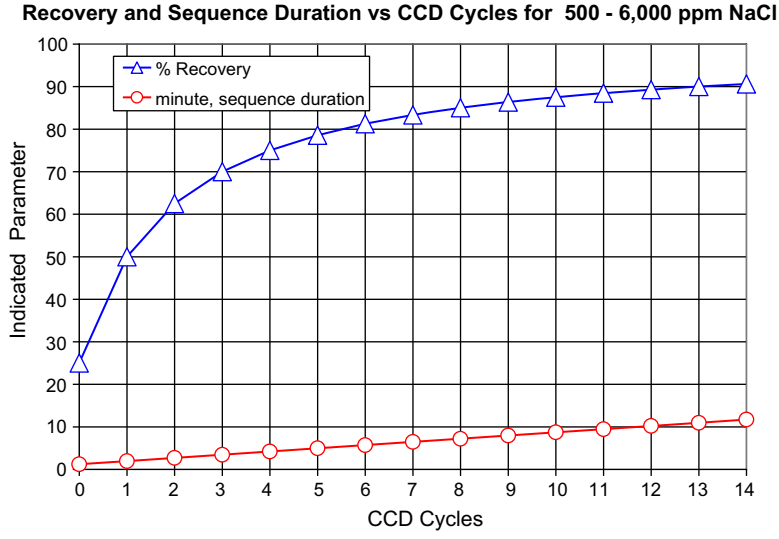

Fig. 19. Recovery and sequence period *vs* CCD Cycles during BWRO-CCD ME4 (E = ESPA2-MAX) simulations with NaCl feed (500–6,000 ppm) under the conditions specified in Table 1.

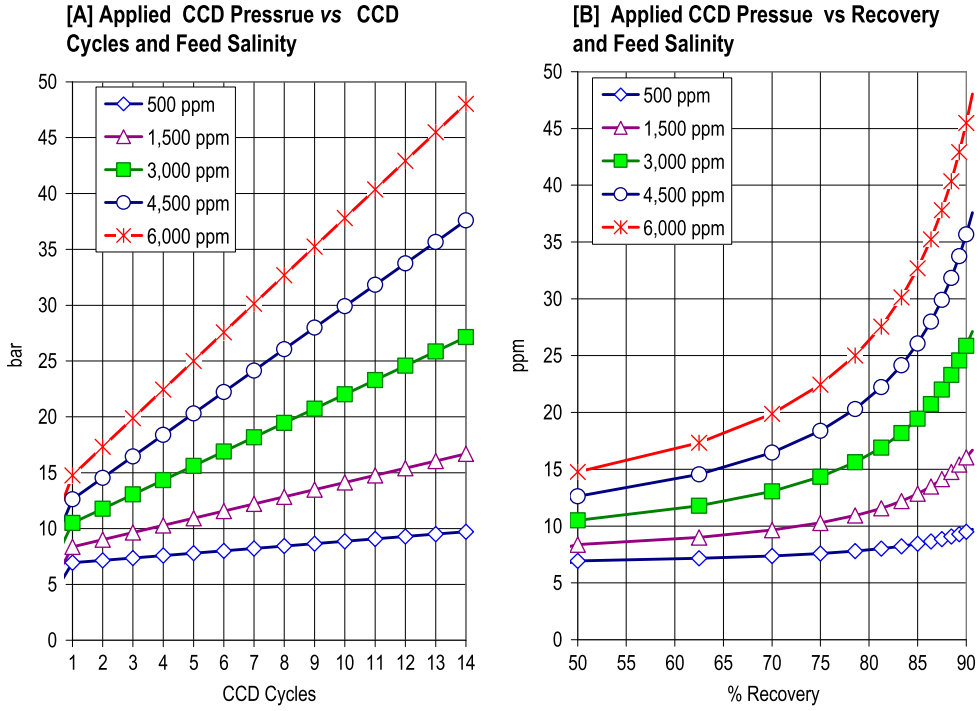

Fig. 20(A–B). Applied CCD pressure *vs* CCD Cycles (A) and recovery (B) during BWRO-CCD ME4 (E = ESPA2-MAX) simulations with NaCl feed (500–6,000 ppm) under the conditions specified in Table 1.

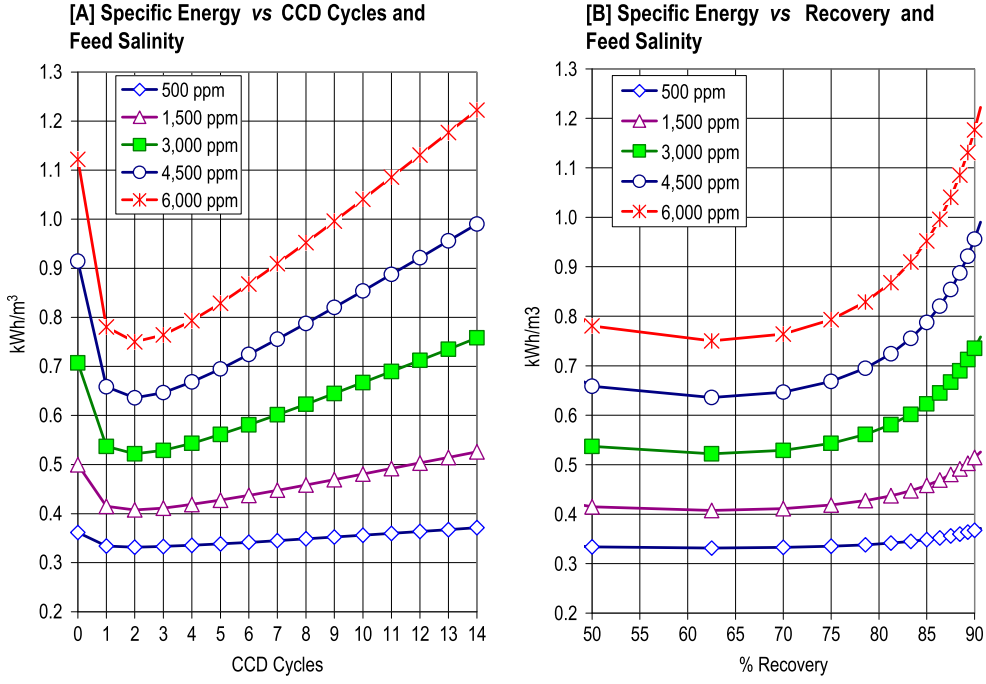

Fig. 21(A–B). Specific Energy *vs* CCD Cycles (A) and recovery (B) during BWRO-CCD ME4 (E = ESPA2-MAX) simulations with NaCl feed (500–6,000 ppm) under the conditions specified in Table 1.

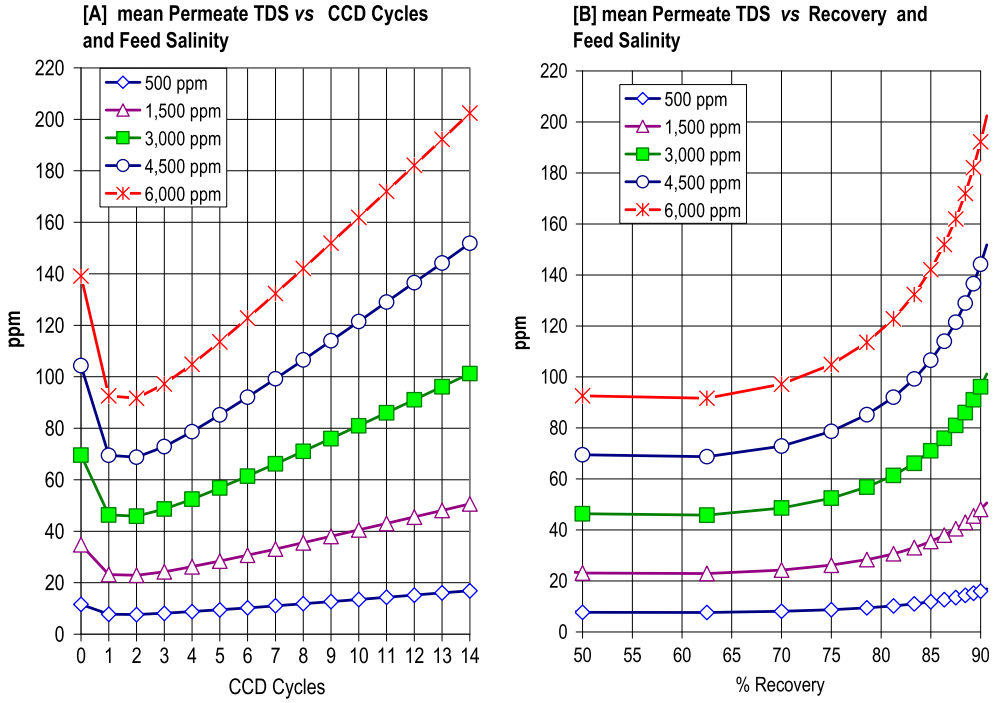

Fig. 22. Permeate salinity (mean TDS) *vs* CCD cycles (A) and recovery (B) during BWRO-CCD ME4 (E = ESPA2-MAX) simulations with NaCl feed (500–6,000 ppm) under the conditions specified in Table 1.

BWRO technique. The low specific energy results without the need for energy recovery means of the model analysis revealed in Fig. 21 are anther manifestation of the progressive pressure rise during CCD cycles along the diagonal instead of the applied pressure needed at the ultimate recovery level by conventional techniques. Noteworthy in Fig. 21(B) is the sharp rise of the mean specific energy with recovery as a function of increased salinity. The average permeate TDS in Fig. 22 manifests the rising cross flow concentrations (C_{CP}) during the sequential progression according to Eq. (3) as function of increased module inlet concentrations (C_f+C_{CP}), since the other parameters in said equation (B, pf_{av}, T_{CF}, and μ) as well as the average element recovery term (Y_{av}) in Eq. (5) remain essentially unchanged when MR is constant.

The SLOPE in Fig. 23 is perhaps the most sensitive criteria for the pressure-boosting ability of HP-vfd whereby fixed flow under variable pressure conditions is maintained throughout the BWRO-CCD process. The theoretical model variations of the SLOPE (bar/%) in Fig. 23(B) and CCD applied pressure in Fig. 20(B) as functions of feed salinity during a sequence of 90% recovery are found to be 0.01–2.29 (6.9–9.5 bar) for 500 ppm; 0.04–6.87(8.4–16.0 bar) for 1,500 ppm; 0.09–13.74 (10.5–25.9 bar) for 3,000 ppm; 0.13–16.70 (12.6–33.7 bar) for 4,500 ppm, and 0.17–22.26 (14.8–42.9 bar) for 6,000 ppm NaCl—the aforementioned is said at flux of 25 lmh and cited feed salinity under the specified conditions in Table 1. The percentage pressure-boosting requirements of HP-vfd for 90% recovery at the flux of 25, according to the aforementioned statement, as functions of feed salinity and SLOPE are illustrated in Fig. 24(A) and (B), respectively, and the results clearly show increased percent of boosting with increased feed salinity with SLOPE being a rather sensitive criteria of such pressure boosting requirements. The efficiency of HP-vfd should not be affected by the variable pressure operation since it takes place with fixed flow rate at a defined efficiency level.

7. Theoretical model assessment of the BWRO-CCD technology

The model analysis provided hereinabove of the BWRO-CCD technology is based on sound theoretical and engineering principles which depart in many aspects from those of conventional techniques and the theoretical model assessment discussed below is intended to focus on the scope and prospects of this noteworthy new advanced technology in the context of the future objectives, goals, and targets of BWRO desalination at large. The majority (>90%) of the commonly practices and/or required RO applications worldwide cover a feed salinity range of 500–6,000 ppm and are intended for water treatment

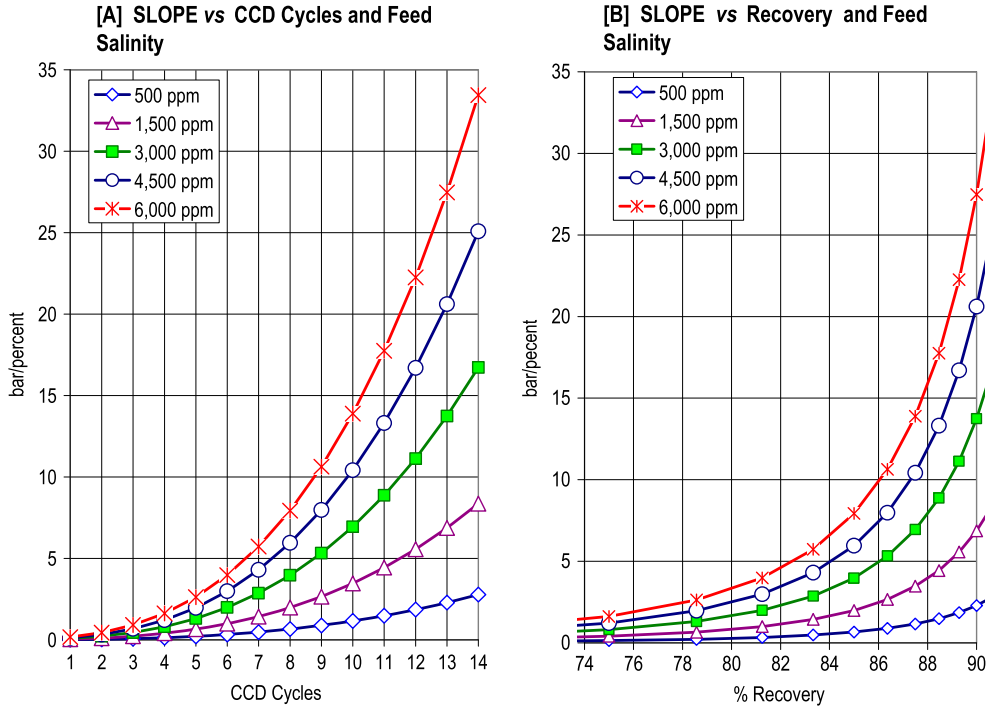

Fig. 23. SLOPE ($\Delta\pi/\Delta$Recovery—bar/%) vs. CCD cycles (A) and recovery (B) during BWRO-CCD ME4 (E = ESPA2-MAX) simulations with NaCl feed (500–6,000 ppm) under the conditions specified in Table 1.

and/or for BWRO of high recovery and low energy consumption with apparatus comprising pressure vessels of 300 psi or 450 psi pressure rating for permeates production with high availability and reduced needs for cleaning. Accordingly, the model analysis assessment hereinafter will focus on aspects related to recovery, energy, and membrane fouling.

7.1. Simple designs of high modularity

The model analysis pertains to a general class of NME*n* (n = 1–6) type BWRO-CCD units comprising N identical ME*n* modules with their inlets and outlet connected in parallel to the same closed circuit and focuses on the ME4 module as exemplified in Fig. 1 for ME4, in Fig. 2 for 5ME4, in Fig. 3 for 10ME4 and in Fig. 4 for 20ME4. The focus on the ME4 configuration is no coincidence since longer modules (n > 4) also imply the lower production contributions of tail elements combined with a declined average flux and increased fouling probability; whereas, modules of four elements could be operated with a relatively higher average flux and enable similar overall production expected of longer modules with better-quality permeates and lower fouling probability. In some cases of low salinity feed with low-scaling constituents, the high recovery applications of the BWRO-CCD technology with modules of five and even six elements is not unreasonable.

The high-modularity design of the units under review is manifested by the number of elements per module (n) and the number of modules (N) per design. The units, each with a single pressurizing pump and a single circulation pump, are designed to perform a continuous consecutive sequential desalination in closed circuit with staged flow rates and pressure boosting without the need of staged pressure–vessels and inter-stage booster pumps as in the case of conventional techniques. Simple desalination systems of high design modularity and superb performance characteristics are projected to play an important role in future BWRO applications.

7.2. Flexible performance of high versatility

Control of the BWRO-CCD process takes place by means of the selection of four principles set points of operation as followed: (1) fixed feed flow rate of HP during PFD steps; (2) fixed feed flow rate of HP during CCD cycles; (3) fixed cross flow of CP during CCD cycles; and (4) maximum applied pressure during CCD cycles. Minor adjustable control settings related to the PFD steps include the brine flow rate control by a manual or an actuated valve means and

the replaced volume of brine by fresh feed, which is essentially that of the free intrinsic volume of the closed circuit with a minor correction to account for some mixing at the interface of the two solutions. The aforementioned set points and control settings are independent of each other and provide an infinite number of control combinations of desired permeate flow or flux during PFD and CCD, desired cross flow, and desired maximum applied pressure. In simple terms, the BWRO-CCD technology under review enables the attainment of any desired recovery at any desired flux with any desired module and head element recovery. The extensive operational flexibility enables ideal process performance optimization tailor-made per each given brackish water feed source.

The operational flexibility and performance variability of the BWRO-CCD technology are fully consistent with the theoretical model analysis simulations results for the ME4 unit at the sequential and/or the continuous consecutive sequential levels according to the data-base in Table 1 and the change of data base, one at a time, whereby the various operational effects could be ascertained and evaluated. The results of theoretical model simulations of the BWRO-CCD system reveal unique performance characteristics such as high recovery selection with low energy consumption irrespective of the number elements per module, flexible selection of flux over a wide range independent of cross flow selection, control of module recovery through the selection of cross flow and pressurized feed flow, and other noteworthy features inconceivable by conventional techniques. The variable operation power characteristics of the BWRO-CCD technology makes it ideal for integration with solar panels and/or wind turbines for desalination by means natural clean renewable energy, since the variable power output of such sources could be directly translated to increased/decreased permeation flux, and thereby enable an uninterrupted desalination operation.

7.3. Low fouling characteristics

The conceptual design of modular BWRO-CCD NME4 systems and their theoretical model simulations are of interest from the stand point of prevention or reduction of membranes fouling, an issue of major concern in many of the BWRO plants around the world. The noteworthy features of the BWRO-CCD technology in the context of fouling reduction are related to the design aspects of short modules and their operational aspects by a controlled two-step (PFD and CCD) consecutive sequential process under fixed flow and variable pressure conditions. Controlled CCD parameters of importance in the context fouling prevention include the flux, cross flow, MR, and maximum operation pressure for reasons specified below.

7.3.1. Prevention of particulate matter fouling not related to scaling

The accumulation of particulate matter inside the pressure vessels in BWRO-CCD is prevented by the frequent fast flush flow of the entire system during the PFD steps of brine replacement with fresh feed, which also removes all particulate matter irrespective of origin. System flush takes place briefly every 10–15 min and the preventions of particulate matter depositions on membrane surface during the CCD intervals is achieved by means of a sufficiently high cross flow selection in order to effect the principle momentum vector of particulate matter maintained in the cross flow direction rather than towards the membrane surfaces. Momentum in the direction of membrane surfaces is enhanced with increased flux, and therefore the relationship between cross flow and flux is also an important feature for the prevention of particulate matter deposition which may be controlled by MR selection, with decreased MR by increased cross flow favoring decreased particulate matter fouling and vice versa. The MR during CCD is determined by the selected operational set points of permeation flow and cross flow which are independent of each other and this provides an excellent tool for the reduction, or even prevention, of particulate matter fouling effect by MR optimization.

7.3.2. Prevention of scaling

Scaling of low-solubility salts during RO is a function of recovery and initiated when the concentrations of ions comprising low-solubility salts exceed their solubility products in saturated solutions. The adding of antiscalant to the feed convert some of the metal ions associated with scaling (e.g. Ca, Ba, Sr, etc.) into soluble complexes, thereby enabling the increase of desalination recovery before the start of scaling. Scaling in conventional PFD techniques is normally associated with tail elements where brine concentration is high and cross flow is slow, and is initiated by crystallized seeds in regions of particularly low cross flow (e.g. inner spaces of pressure vessels surfaces near elements) which induce fast scaling. The theoretical model analysis of the BWRO-CCD system according to the database in Table 1 suggests the low-scaling characteristics of this technology for the following reasons:

(1) During the CCD cycles of the process the concentrate is recycled and diluted with fresh at inlet to module(s) and this dilution effect inhibits the formation of crystallized seeds to an advanced recovery level as a function of the selection of cross flow, MR, maximum applied pressure, and antiscalant, as well as function of the number of elements per pressure vessel in the design. Process optimization by set points selection combinations in the absence of adverse effects typical of tail elements in longer modules as in conventional techniques, should allow the attainment high recovery before the appearance of crystallized seeds which trigger fast scaling.
(2) A smaller number of elements per pressure vessel in BWRO-CCD units compared with conventional techniques generally implies the ability to maintain a faster cross flow with lower MR, and therefore reach the desired recovery with a larger number of CCD cycles. A larger number of CCD cycles under said conditions imply a safer reach of the ultimate maximum recovery of a given feed sources just before crystallized seeds appear and scaling becomes unavoidable. Even if crystallized seeds start to appear near the desired recovery of the BWRO-CCD unit their scale triggering effect is avoided during the PFD flush step in the process which removes all particulate matter including the small crystallized seeds if formed.
(3) The cross flow and MR in BWRO-CCD are fully controlled by operational set points, which can be changed online, and thereby provide an effective tool to reach the desired recovery with a sufficient number of CCD cycles and cross flow of minimum probability for crystallized seeds formation which induce scaling. In simple terms, this approach enables the optimization of the process for each specific brackish water source depending on its compositions in reference to scaling, and this is irrespective of the number of elements per pressure vessel.
(4) The selection of an appropriate antiscalant for a specific feed source of a defined composition implies the ability to increase the recovery to a level predicated in advance by use of computer analysis programs of antiscalant producers. It should be pointed out that the antiscalant computer programs are intended for the stationary-state conditions of the tail elements in pressure vessels of conventional techniques, wherein the average cross flow and flux are relatively low and steady and the inlet and outlet concentrations remain unchanged. In contrast with conventional techniques, the average cross flow and flux in BWRO-CCD modules are controlled at desired high levels with much smaller margins between head and tail elements. The cross flow sequential concentration variations between minimum and maximum as functions of CCD desalination progression may be expressed on the time scale as exemplified in Figs. 9–13 for a typical continuous consecutive sequential process. The development of suitable antiscalant computer programs for the BWRO-CCD technology will most probably reveal considerably higher maximum recovery prospects compared with conventional techniques in light of less-favored conditions for crystallized seeds' formation at the final sequential CCD cycle in the process. Crystallized seeds formation at the final cycle of the BWRO-CCD process does not necessarily imply scaling, since the fast flush flow of the entire system with fresh feed by PFD immediately after the desired recovery is attained will remove all particulate matter from the system, including crystallized seeds if formed, and thereby avoid the triggering of scaling and enable the start of a new sequence in the absence of triggering factors of scaling.

7.3.1. Bio-fouling prevention

The conditions prevailing inside modules of the closed circuit BWRO-CCD units, in particular the sufficiently fast cross flow combined with the large consecutive sequential salinity variations of the recycled concentrate during the CCD cycles of the consecutive sequential process, are not conducive to bacteria growth which normally starts inside pressure vessels where flow is limited and salinity remains unchanged. The fast cross flow created inside the short ME4 modules combined with the frequent and large salinity variations of cross flow (e.g. ten fold salinity increase of feed at 90% recovery) and the brief fast flush flow during PFD steps every 10–15 min reduce or eliminate the probability for bio-fouling in such a system from the theoretical stand point.

7.4. Diverse feed sources applications including variable salinity sources

Practical BWRO applications are normally experienced with constant salinity feed sources of up to 6,000 ppm with common scaling constituents (e.g. sulfate, calcium, barium, etc.) which limit the desalination recovery (≤90%) prospects of such systems. The most common conventional approach to the desalination of brackish water is by means of two-stage units equipped with turbochargers for effective recovery of up to 85% with reasonable energy consumption. The conventional approach is limited to sources of small salinity variability since it is confined by designed for specific operational conditions of near-constant applied pressure. In contrast with conventional techniques, the BWRO-CCD approach implicates simple modular designs of staged flow and pressure-boosting characteristics not confined to specific operations conditions nor to a narrow applied pressure range and may apply to diverse feed sources, which according to the theoretical model analysis, covers the salinity range of up to 7,000 ppm defined by the equivalent of 6,000 ppm NaCl. The aforementioned salinity range limit manifests according to the theoretical model analysis of the boosting pressure ability of ordinary pressurizing pumps (HP-vfd) to reach high recovery desalination with common pressure vessels of 450 psi maximum pressure rating. The BWRO-CCD is a variable pressure technology of flexible maximum applied pressure selection which may be applied for the desalination of feed sources with changing salinity. According to the theoretical model analysis of the BWRO-CCD ME4 model, the set point of maximum sequential pressure dictates the recovery of a defined salinity feed source and when neither this set point nor any of the other set-points of operation in the system are changed, while the salinity of the feed source changes, this will be prompt change is recovery. In simple terms, a defined set point of maximum applied pressure will automatically perform with high recovery when the feed source salinity drops and with lower recovery when the feed source salinity increases with the magnitude of recovery changes manifesting the extent of salinity changes.

7.5. Divers application prospects of low energy and high recovery

The theoretical model analysis results of the BWRO-CCD simulations in Figs. 19–24 for the feed range of 500–6,000 ppm NaCl suggest the unlimited application prospects of this technology for high recovery and low energy desalination for most of the common brackish water sources with up to 7,000 ppm, equivalent to 6,000 NaCl. Such application prospects are noteworthy in particular when coupled

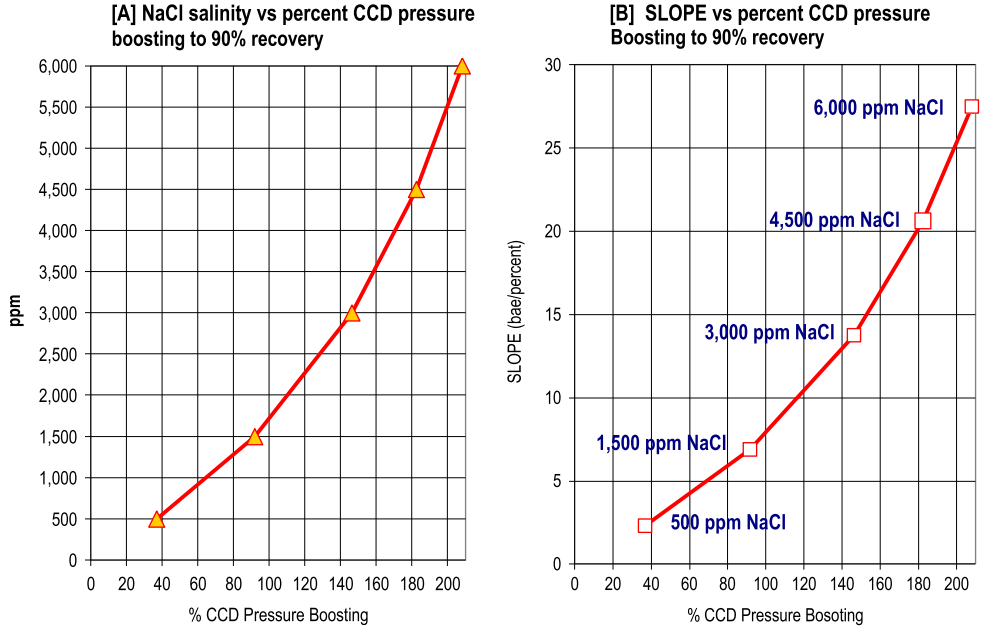

Fig. 24. CCD pressure boosting percent of HP-vdf to 90% recovery at flux of 25 lmh SLOPE as function of NaCl feed salinity (500–6,000 ppm) in (A) and SLOPE in (B) during the BWRO-CCD ME4 (E = ESPA2-MAX) simulations under the conditions specified in Table 1 except for cited feed concentration.

with low fouling characteristics (Section 7.4), simple designs of high modularity (Section 7.1), and flexible performance of high versatility (Section 7.2), a combination not possible by any other existing technique. The broad spectrum of applications includes, for instance, treatment of surface and groundwater domestic supplies, desalination of clean domestic and industrial effluents, desalination of brackish water, desalination of feed sources of changing salinity, high-quality permeate supplies to industry, and decontamination of drinking water, such as effective nitrate removal under high flux conditions and boron removal from SWRO permeates, as well as many additional applications.

8. Theoretical model assessment support by BWRO-CCD performance results

The BWRO-CCD technology was initially conceived on the basis of model simulations and since inception the growing volume of experimental data was found to be fully consistent with model simulations, this has enabled the development of a reliable uniform design approach of units by this technology which operate on the basis of different conceptual principles compared with convention techniques. Conventional design computer programs of membranes producers could only assist in analyzing specific steps in the CCD process but cannot apply to the entire process.

Experience gained with the CCD technology started in 2006 with the BWRO-CCD ME3 experimental pilot in Rannana, Israel, which was tested with domestic water supplies of 555 ppm TDS, 1,010 μS/cm, pH = 6.9, 420 ppm hardness ($CaCO_3$), 88 ppm NO_3, and 37 ppm silica and was intended to evaluate the applicability of new technology for feed softening and nitrate removal. The Rananna trials [21] with BW30LE-44O elements were carried out in the fixed feed/permeate flow range 3.7–6.4 m^3/h (30–51 lmh) with fixed cross flow of 8.5 m^3/h (module recovery range: 29–41%) under variable CCD applied pressure conditions with the maximum in the range of 11.6–17.6 bar for recovery of 89 ± 1.5%. Several brief pilot trials were also performed using CPA3 elements under fixed pressure (max., 19.5 bar) and variable feed flow (e.g. 5.0–3.5 m^3/h; 45–30 lmh) conditions with up to 93.5% recovery.

The field track record of the BWRO-CCD technologies started in the beginning of 2009 with the 8ME4 [16] and 10ME4 [15] units at Reim, Israel, and more than additional 20 units were installed in Israel and elsewhere (USA, Singapore, Spain, and India) [17,18]. The application of the CCD technology to Mediterranean seawater was initiated in the beginning of 2011 with four different 4ME*n* (n = 1–4) experimental prototypes [11–13], and more recently this technology was also demonstrated for ocean seawater in a Caribbean site.

The performance records of many of the aforementioned CCD units are described at length in the literature [11–19] ith revealed experimental results fully support the various theoretical model assessments and projections made hereinabove with regard to the advantages and benefits of the CCD technologies at large and the BWRO-CCD technology in particular.

9. Concluding remarks

The study under view presents a comprehensive theoretical overview of the newly emerging BWRO-CCD and its simple design features and flexible performance of low energy and high recovery consumption with reduced fouling characteristics which meet the criteria of advanced desalination technology. The results of this theoretical study which are fully consistent with experimental data collected thus far may suggest the feasibility of BWRO-CCD becoming the technology of choice for most BWRO applications for wide a range salinity feed sources where saving of energy and high recovery are important desired features. The new BWRO-CCD technology is a variable pressure technology of variable power demand and as such particularly suitable for direct integration with solar panels and/or wind turbines for clean renewable power utilization for desalination which may provide solution for drinking water needs in large global regions where grid electricity is not available and electricity generated by diesel engine is too expensive.

Acknowledgments

Funds to *Desalitech Ltd*. by the AQUAGRO FUND L.P. (Israel) and by Liberation Capital LLC (USA) are gratefully acknowledged.

References

[1] Waterlines Report Series No 9, Emerging trend in desalination: A review, UNESCO Centre for Membrane Science and Technology, University of New South Wales, Commissioned by the National Water Commission, Australian Government, October 2008. Available from: http://www.nwc.au/_data/assets/pdf_file/0009/waterline_-Trends_in_Desalination-_REPLACE-2.pfd

[2] M. Elimelech, W.A. Phillip, The future of seawater desalination: Energy, technology, and the environment, Science 333 (2011) 712–717.

[3] N. Voutchkov, Membrane seawater desalination—Overview and recent trends, IDA conference, November 2–3, CA, US, 2010.
[4] N. Voutchkov, R. Semiat, Seawater desalination, in: N. Li, A.G. Fane, W.S. Ho, and T. Matsuura (Eds.), Advance Membrane Technology and Applications, John Wiley, New Jersey, NJ, 2008.
[5] L.F. Greenlee, D.F. Lawler, B.D. Freedman, B. Marrot, P. Moulin, Reverse osmosis desalination: Water sources, technology and today's challenges, Water Res. 43 (2009) 2317–2348.
[6] L.M. Camacho, L. Dumée, J. Zhang, J. Li, M. Duke, J. Gomez, S. Gray, Advances in membrane distillation for water desalination and purification applications. Rev. Water 5 (1) (2013) 94–196.
[7] J.P. MacHarg, Principle Investigator, Energy optimization of brackish groundwater reverse osmosis desalination, Final Report for Contract Number 0804830845, Texas Water Development Board, Austin, TX, September 2011, 78711–78711.
[8] P. Zhang, J. Hu, W. Li, H. Qi, Research progress of brackish water desalination by reverse osmosis, J. Water Resour. Prot. 5 (2013) 304–309.
[9] Dow Liquid Separation, FILMTECTM Reverse Osmosis Membranes, Technical Manual as an example 2011. Available from: http://msdssearch.dow.com
[10] S. Loeb, S. Sourirajan, American Chemical Society Advances in Chemistry Series, ACS 38 (1963) 117–132.
[11] A. Efraty, N.R. Barak, Z. Gal, Closed circuit desalination - A new low energy high recovery technology without energy recovery, Desalin. Water Treat. 31 (2011) 95–101.
[12] A. Efraty, N.R. Barak, Z. Gal, Closed circuit desalination series no-2: New affordable technology for sea water desalination of low energy and high flux using short modules without need of energy recovery, Desalin. Water Treat. 42 (2012) 189–196.
[13] A. Efraty, Closed circuit desalination series no-6: Conventional RO compared with the conceptually different new closed circuit desalination technology, Desalin. Water Treat. 41 (2012) 279–295.
[14] R.L. Stover, N. Efraty, Record low energy consumption with closed circuit desalination, IDA World Congress—Perth Convention and Exhibition Center (PCEC), Perth, Western Australia, September 4–9, 2011, REF: IDAWC/PER11-375.
[15] A. Efraty, Closed circuit desalination series no-3: High recovery low energy desalination o brackish water by a new two-mode consecutive sequential method, Desalin. Water Treat. 42 (2012) 256–261.
[16] A. Efraty, Closed circuit desalination series no-4: High recovery low energy desalination of brackish water by a new single stage method without any loss of brine energy, Desalin. Water Treat. 42 (2012) 262–268.
[17] A. Efraty, Z. Gal, Closed circuit desalination series no 7: Retrofit design for improved performance of conventional BWRO systems, Desalin. Water Treat. 41 (2012) 301–307.
[18] A. Efraty, J. Septon, Closed circuit desalination deries no-5: High recovery, reduced fouling and low energy nitrate decontamination by a cost effective BWRO-CCD method, Desalin. Water Treat. 49 (2012) 384–389.
[19] R.L. Stover, Industrial and brackish water treatment with closed circuit desalination reverse osmosis, Desalin. Water Treat. 51 (2013) 1124–1130.
[20] A. Efraty, Continuous closed-circuit desalination apparatus without containers, US Patent No 7,695,614.
[21] Desalitech Ltd, Unpublished results.